# 3. AIM OF THE WORK

In the present work, a new digital stethoscope system will develop for diagnosing and monitoring lung and heart diseases. The aim of the present work is to improve the instruments performance, determine parameters relevant to disease detection within the lungs and the heart.

4. MATERIALS AND METHODS

The present thesis utilizes a combination of two different techniques to aid determination of condition of heart and lung. The first technique is a passive digital stethoscope which involves listening, computer recording and analysis of natural heart and lung sound. The second technique involves actively introducing an audible sound signal into the lungs and monitoring the signal after passes through some portion of the patient lung by using the digital stethoscope.

4.1 Schematic diagram of the passive technique (designed digital stethoscope):

The proposed stethoscope system used in the present work is shown in (Fig 24). It consists of a traditional stethoscope, a microphone, an amplifier and filter circuit to process the signals generated m a sound card, a headphone, interface and personal computer (PC) for further processing by the software. The analog heart and lung signals from the electronic stethoscope were stored and uploaded offline to a digital oscilloscope and PC for further analysis.
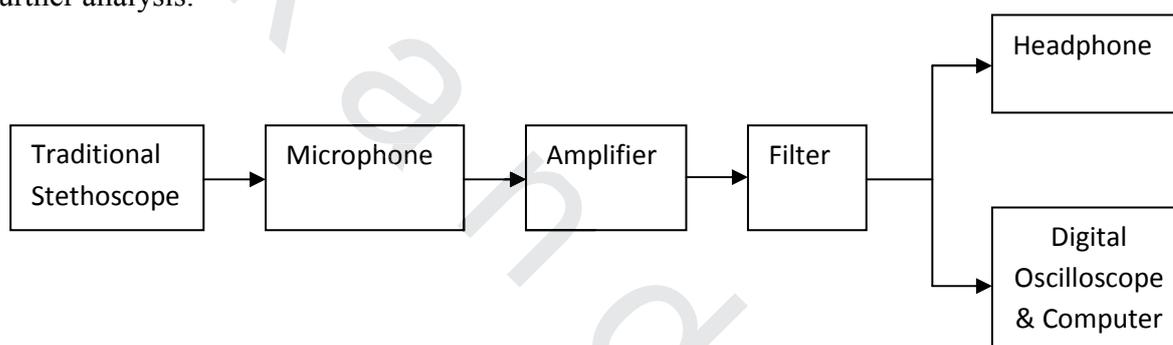
Fig. 24: Block diagram of the designed system

The captured electrical signal received by microphone is amplified using an analog amplifier circuit before encoding for transmission via the transmitter. Fig. 25 shows the microphone biasing and amplification circuit in the chest-piece. The circuit was designed using Multisim design suite of National Instruments. The electret microphone was designed to have a biasing voltage of 2 V for the operation of the incorporated field effect transistor, which is consistent with the conventional electret microphones. With a power supply, V2 of 3.0 V, resistor R1 of 1.0 kΩ and internal resistance, Rs, of the electret microphone (2.2 kΩ based on manufacturer datasheet) the required bias voltage was obtained. An active low pass anti-aliasing filter with a cut-off frequency, fc of 3 kHz and a gain of 25.5 dB was found adequate to ensure that the sampling theorem was obeyed. To minimize attenuation effect at low frequency, de-coupling and DC noise rejection capacitors (C2, C4, C5) shown in the circuit in (Fig. 25) were chosen to be sufficiently high (10 μF). The second stage amplifier circuit, U2A, was employed to produce an inverted output signal with unity gain. The output together with its inversion served as a differential input to the wireless transmitter circuit. This ensured that the output is less susceptible to interference as the difference remains the same despite voltage spikes in both lines.
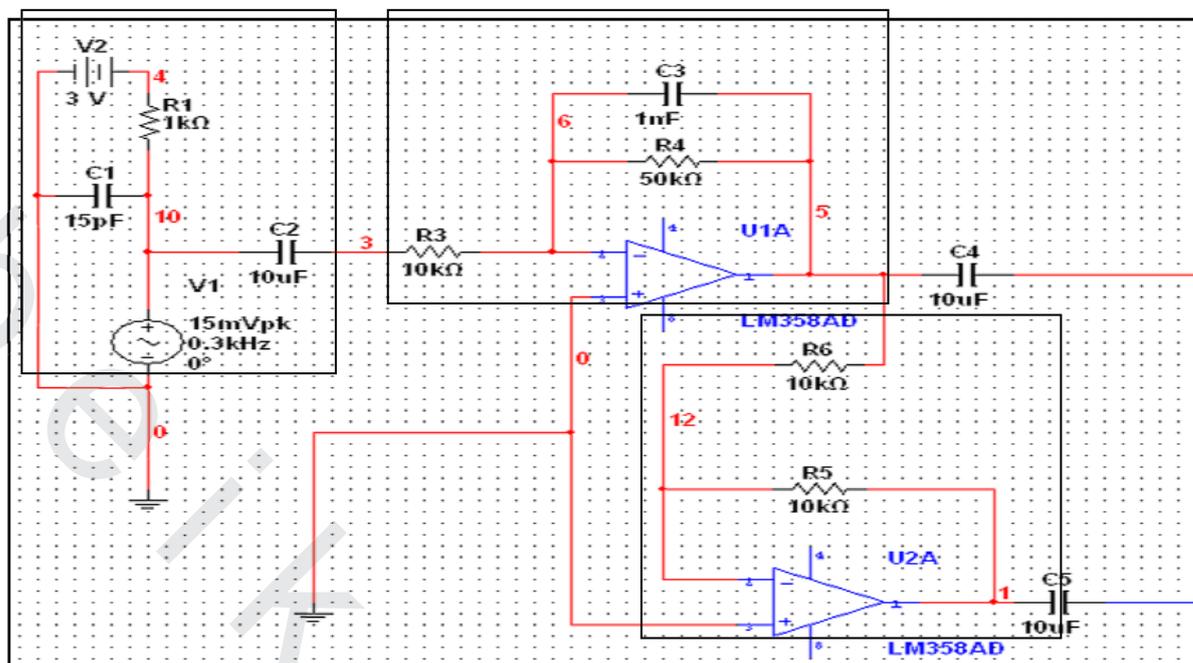
**Fig. 25**: Microphone bias, low pass filter and the pre-amplification circuit

The preamplifier and filtering circuit is operated by the same two series Zinc-Carbon batteries 9v for supplying the circuit with 18v DC. The circuit consists of two channels; the signal was picked up by an electrets condenser microphone connected with the stethoscope chest piece to the input of the circuit.


Fig. 26: digital storage stethoscope

The sound signal received by the two electrets condenser microphone to the constructed preamplifier and filter circuit for processing the sound signal to a digital storage oscilloscope (Instek GDS-820) (Fig. 26) and software analysis using personal

computer. The printed circuit board of the amplifier and filter circuits is shown in Fig. 27. Photo of complete digital stethoscope system is given in Figure 28.
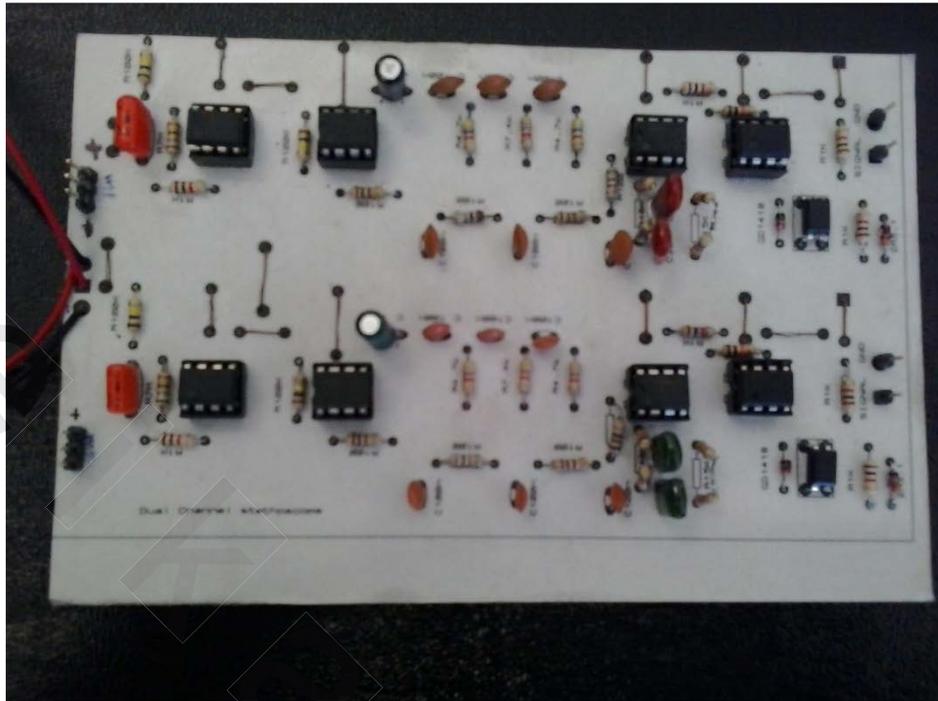
Fig. 27: preamplifier and filtering circuit
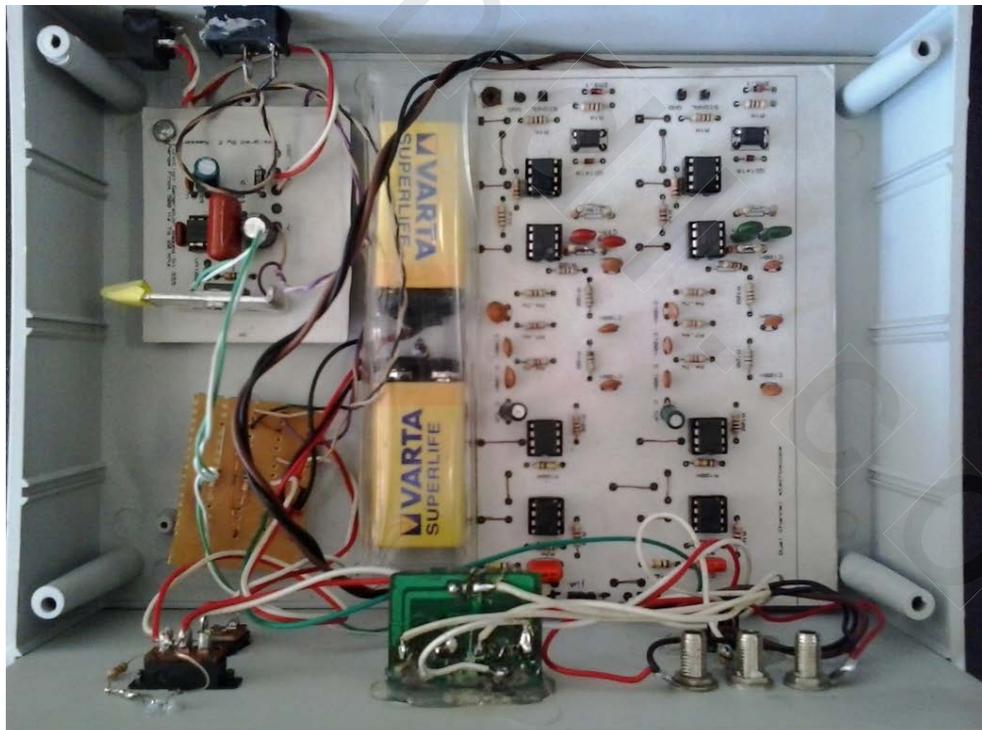
Fig. 28: Photo of complete Stethoscope System.

4.2 Sensor:

Condenser microphones and piezoelectric accelerometers have been recommended. Both transducers are popular in sound recording. However, accelerometers are typically more expensive than microphones, are often fragile, and may exhibit internal resonances. Thus, this concludes that the microphone is perfect for the application.

Condenser microphones generally have flatter frequency responses than dynamic, and therefore mean that a condenser microphone is more desirable if accurate sound is a prime consideration as required in this design. There are two types of condenser microphones; standard condenser and electret condenser. A standard condenser microphone consists of a small diaphragm that vibrates in response to acoustic pressure. Standard condenser microphones have very high output impedance, so they are not suitable for transferring signals over even a very small distance. An electret condenser microphone (fig ٢٩) combines a condenser microphone with a Field Effect Transistor (FET), which amplifies the signal and transforms the impedance to a more useful level. This characteristic of electret condenser microphones makes them very sensitive to small sounds.
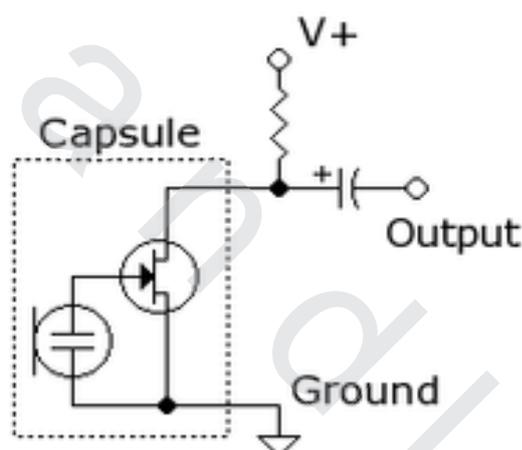

Fig. ٢٩: equivalent circuit of the electrets condenser microphone

The simplest and least effective method of sound detection was achieved by placing a microphone in the chest piece. This method suffers from ambient noise interference and has fallen out of favor. In the present work to eliminate interference a sensor consists of three parts: Diaphragm, Condenser microphone and 2.5 mm audio plug was used. Sound waves from the acoustic amplifier (diaphragm) are fed to the condenser microphone. The sound waves hitting the condenser microphone change its capacitance by changing its impedance, which produces a voltage swing proportional to the amplitude of the input sound waves. The voltage swing of the signal also depends on the bias voltage given for the microphone. A microphone bias voltage of 1.25 V is produced by the audio codec. The coupling of the acoustic sensor to the microphone is critical to pick up noise free sound signals from the human body.

Place the microphone as close as possible to the diaphragm; the microphone should be connected to a 2.5 mm plug to connect the 2.5 mm jack to the front-end board. The

electric wire that connects the microphone to the plug is made long enough to ensure that there is sufficient length to place the sensor on the subject (Fig. ٣٠)
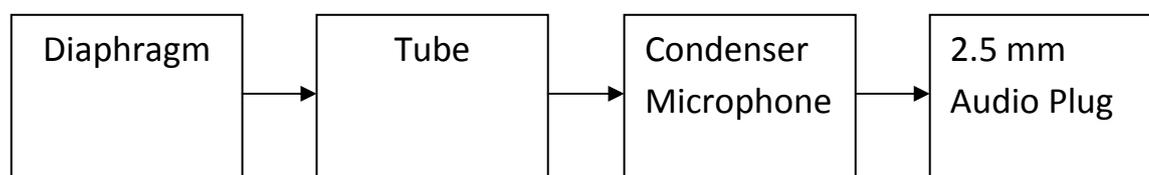
Diaphragm	→	Tube	→	Condenser Microphone	→	2.5 mm Audio Plug

Fig. ٣٠: Sensor Coupled Microphone

The electret condenser microphone operating voltage is 3v, operating frequency ranged from 20Hz to 20 KHz, and operating temperature from -20c to 70c. It employs the principle of electrostatics and consequently, requires voltage supply across the capacitor for it to work, It is not ideal for high volume work as its sensitivity makes it prone to distortion. This characteristic of electret condenser microphones makes them very sensitive to small sounds.

The basic procedure is to use a resistor between the voltage source and ground to limit the current into the FET, and a capacitor to block the DC offset of the supply voltage from the preamplifier circuit. Two microphones were used in the constructed system connected by a short silicon tube to the chest piece of an acoustic stethoscope (fig. ٣١).
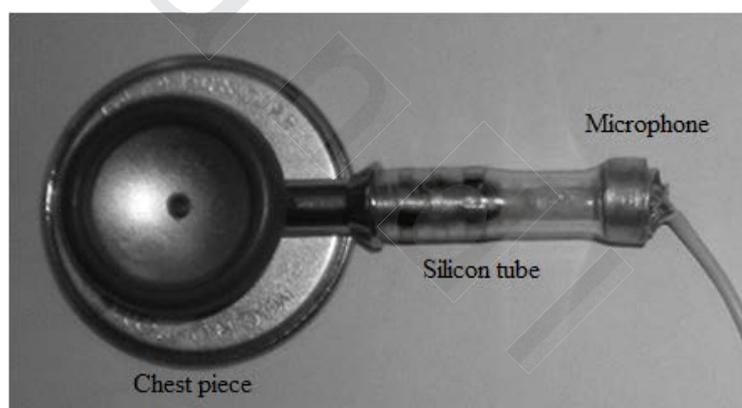
Fig. ٣١: connections of the microphone to the chest piece

4.3 Active Technique for the Determination of Lung Condition:

This part describes the instrumentation aspects of a medical instrument developed in this thesis that measures changes in the distribution and density of lung fluid. The instrument uses a sound signal to excite the respiratory system and measures it on the surface of the chest using an array of electronic stethoscopes in order to develop a sound propagation model of the chest. To examine this technique pre experiments was carried out on a balloon model (simulated lung model) which will be explained.
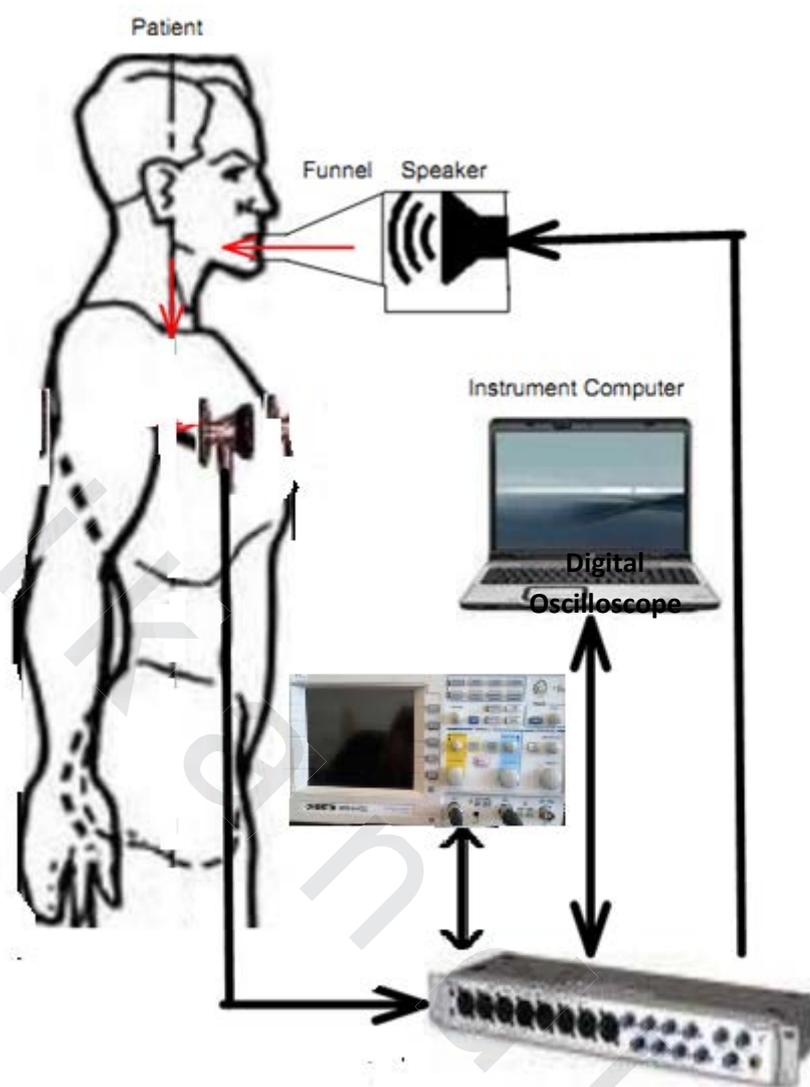
Fig. 32: Sketch of Measurement Apparatus and Setup on a Patient

The active technique instrumental setup shown in Fig. ٣٢ was designed to emit a sound into a patient's mouth and measure the sound on the posterior surfaces of the chest using digital stethoscope placed on the chest. For the sound emitting component of the data acquisition process a White Gaussian Noise (WGN) input signal spread over the frequency spectrum of $0 - 4$ kHz was generated using signal generator. The signal received by the stethoscope is amplified and filtered, processed using a digital storage oscilloscope and software analysis using personal computer.

4.4 Signal generator circuit:

The audible generator used in the present work consists of electrical signal generator and mini speaker. The electrical signal generator circuit (Fig. ٣٣) used for providing an AC signal of adjustable amplitude and varying frequency. The circuit is powered using the supplied 18 v from dc power supply or external two batteries. The complete speaker system is shown in Fig.٣٤. It contains an electronic oscillator that generates sinusoidal oscillations of desired frequency; it can produce oscillations ranging from 20 Hz to 5 KHz.

Microcontroller unit (MCU) (PIC16f627A) was used to generate various waveforms and frequency adjustment. The signal frequency was adjusted at 700 Hz in a sawtooth waveform as an input for the mini- speaker which injects sound to the simulated lung model. The function generator circuit operated by two series Zinc-Carbon batteries 9v for supplying the circuit with 18v DC. 3D printed circuit board of the signal generator is shown in Fig. ٣٤.

(a)

(b)
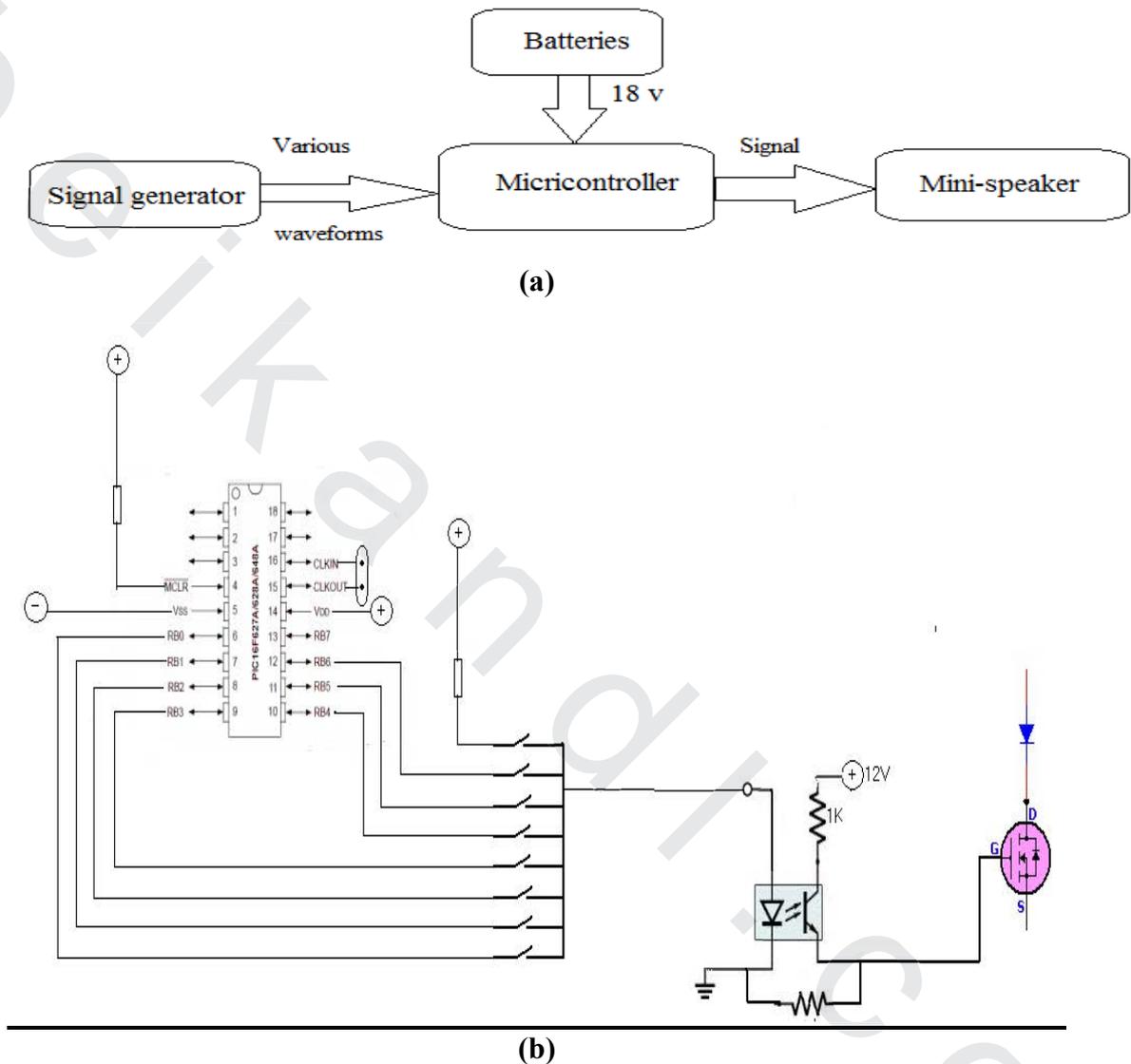
Fig. 33: signal generator circuit : (a) block diagram and (b) circuit diagram
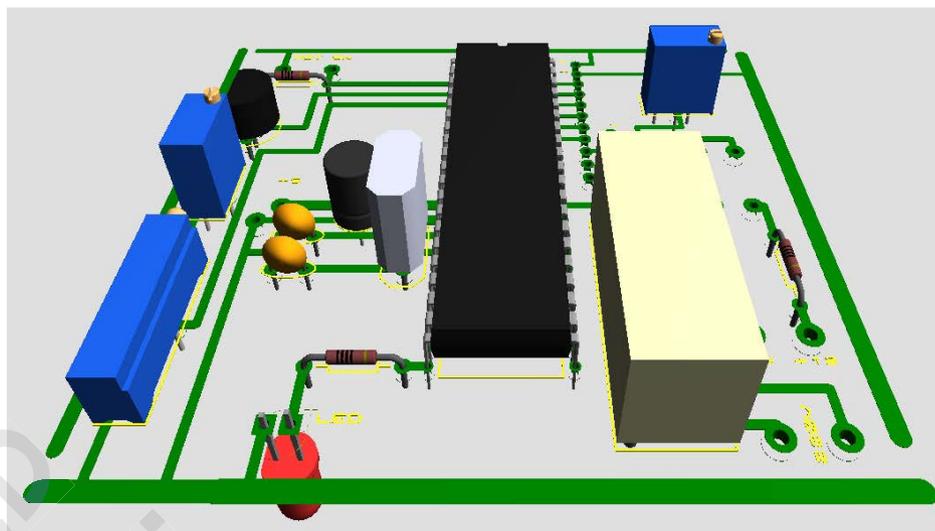
Fig. 34: 3D simulation of signal generator circuit

4.5 Microcontroller:

Microcontroller is one of the most important developments in electronics since the invention of the microprocessor itself. No other external components are needed for its application because all necessary peripherals are already built into it like memory unit, timer unit, and analog to digital converter.

4.5.1 Analogue Interfacing (Fig 35):

Many control applications require the measurement of analogue variables, such as voltage, frequency, attenuation and so on. The PIC microcontroller like any digital circuit cannot understand analog values, only logic One and Zero. The A/D allows conversion of an analog input signal to a corresponding digital representation. The analog voltage enters via an A/D channel then transferred to a Sample and Hold module. The output of the sample and hold is the input into the converter, which generates the result via successive approximation.
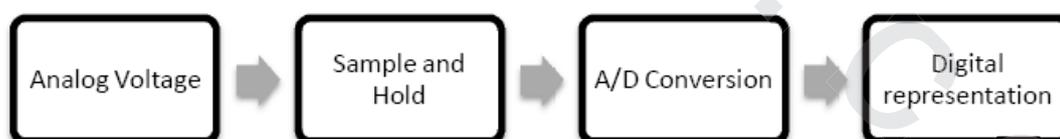
Fig. 35. Block diagram of Analogue Interfacing via Microcontroller

4.7 The balloon Lung Phantom Model:

The lung phantom model was incrementally developed to both verify algorithm implementations of adaptive filtering and to simulate human lung behavior to sound signals. The final lung model that was developed was used to test the instruments ability to detect changes in sound propagation delay with changes of water volumes within the system. The instrument' ability to localize the excess volume of water was also tested. It

consists of a balloon filled with a suitable amount of air (Fig. 36). A mini-speaker placed at one end of a silicon tube which simulates the human trachea and the other end connected to the balloon which simulates the human lung. Two chest pieces of an acoustic stethoscope connected to two electrets condenser microphones; one was placed under the balloon, and the other placed at one side of the balloon.
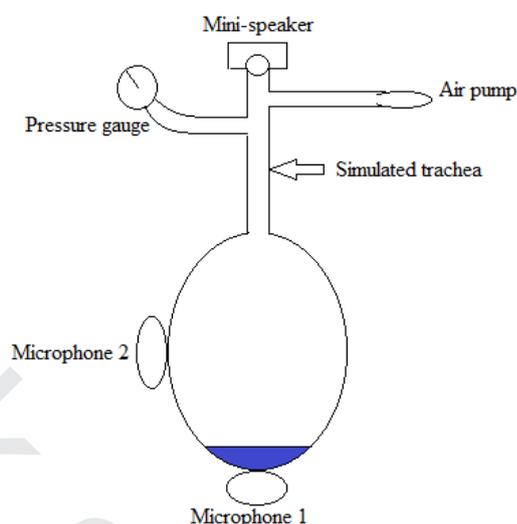
Fig. 36: The simulated lung Phantom and trachea model

The input sound signal was injected into the simulated trachea by the mini-speaker and received it by the array of the chest pieces of the stethoscope, the frequency of the input signal varied from 400Hz to 1500Hz for each medium (water and ultrasonic gel) applied from the designed function generator circuit with various waveforms to know the optimum input frequency and waveform that deals with different mediums used in the experiment.

The balloon filled with air to a pressure of 30 mmHg, applying different sound frequencies from 400Hz to 1500Hz increment by 100Hz with sinusoidal, sawtooth, and square waveforms for each input frequency at an input voltage of 8v. Volumes of water are 15, 25, 40, 50, 65, 75, 90, 100, 110 ml. Due to gravity, water injected into the balloon flowed to the bottom of it, accumulated over microphone 1.

4.7.1 Ultrasound gel:

The experiment was repeated using ultrasound gel for simulating the mucous that may found in patients with obstructive lung diseases with volumes of 25, 50, 75, 100 ml. The pH of the human lung fluids is about 7 -7.5 [104- 106].

4.7.1.1 Specification of the ultrasound gel:

- Composition: Water, polymer, neutralizer, and preservative.
- pH range: 6.5 – 7.5
- Density: 1.03 (g/cm3). Range 1.02 to 1.04.
- Viscosity: 80,000 – 100,000 cps

4.7.2 Solution concentrations:

The same procedure was done with different solutions (sodium chloride NaCl, Glucose), and different concentrations for each solution. The concentrations used are 1%, 5%, 10%, 20%, 30%, and 40%. Each solution and concentration was tested with various frequencies and different waveforms.

4.8 Data acquisition:

4.8.1 Real heart and lung sounds:

The heart sounds used for this study were downloaded from university of Michigan website, and lung sounds from 3M™ Littmann® Stethoscopes website. The collected heart sounds were recorded with length of 30 seconds, and were auscultated from all four auscultation points with normal and abnormal heart sound of each auscultation point. The information regarding the acquired signals is however limited to the presence of a murmur and its temporal location (systole/ diastole).

Fig. 37: The four auscultation points of the heart

The .wave file was read and played using Media Player 3 (Mp3). The sounds are generated from a mini-speaker and recorded by an electret condenser microphone connected to the chest peace of the designed digital stethoscope system for further amplification and filtration, interfaced to a computer for certain modification and analyzed using Multi track audio editor (Audacity) software.

Fig. 38: The user interface

Fig. 38 shows the user interface of the software program. The user interface has buttons for record, pause, rewind, play, and stop. When the sound source is ready, just hitting the record button for recording the sound signal in the time domain waveform.
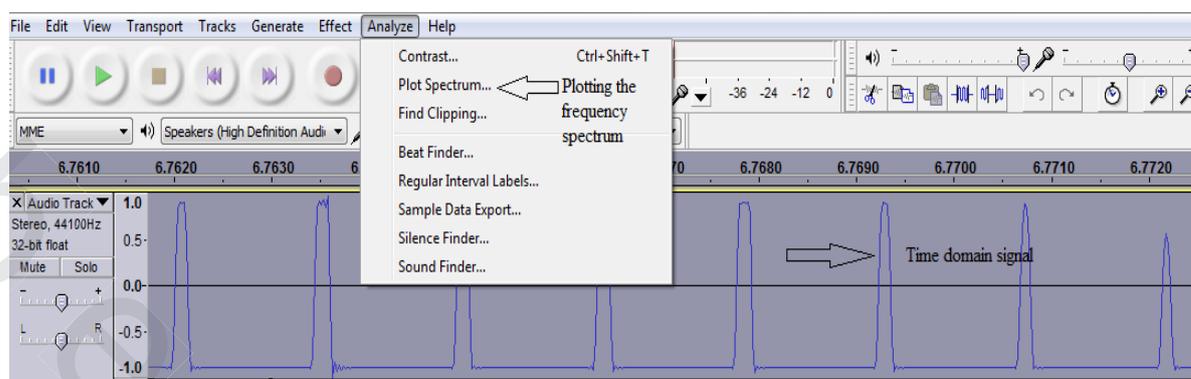
Fig. 39: analyzing the time domain signal

The Fourier transform of the waveform reveals its frequency components and can be computed by highlighting a region of the waveform and selecting the menu item "Analyze -> Plot Spectrum" which produces the result shown in (Fig. 40) below. Using the cursor reveals the tallest peak at 20938 Hz.
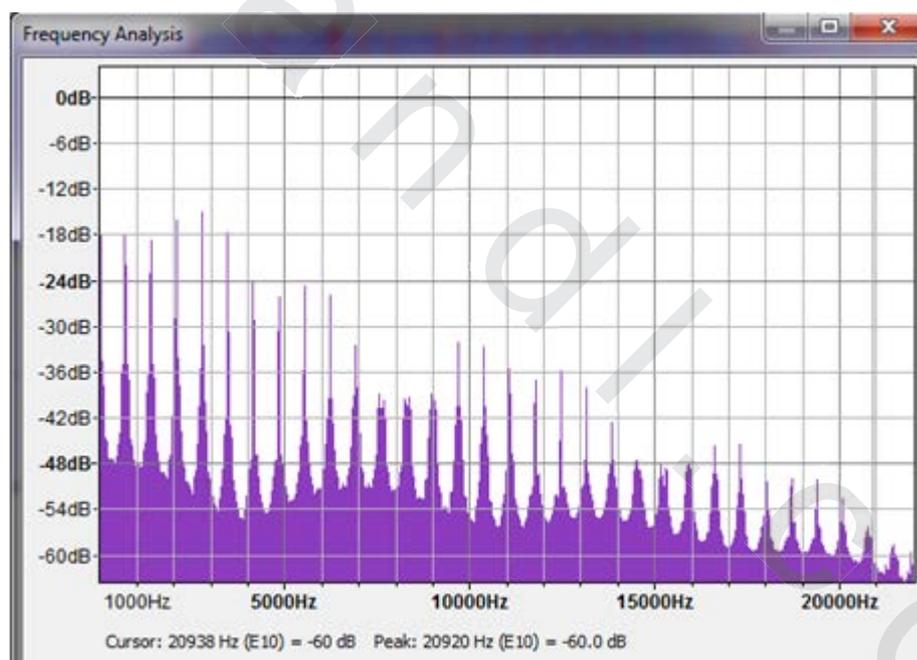
Fig. 40: The frequency spectrum

5. RESULTS

In the present work, a digital stethoscope system is designed and constructed for diagnosing lung and heart diseases. The system proposed has been successfully implemented in effective monitoring and diagnosing of heart and lung sound abnormalities. Real time acquisition of the lung and heart sound has been possible with minimum noise. The heart and lung sound is picked using a stethoscope collected from dispensary and an electrets microphone. Then signal is amplified and filtered using an instrumentation amplifier of gain 1000V/V and a band pass filter with a cut off frequencies of 20-1500Hz. This signal can be recorded using AUDACITY software and can be stored as a dataset. This software records the heart and lung sounds and displays it when required. To obtain the heart signal in the frequency domain the Fast Fourier Transform (FFT) was recorded using the digital oscilloscope or calculated using a MATLAB computer program Human heart and lung signals are detected by using a simple microphone through a personal computer; the signals are recorded and analyzed. Amplitude and frequency analysis are carried out for various pathological cases. The measurements can be saved for further analysis.

5.1 Applications of Passive Technique for the Analysis of Heart and Lung Sound:

5.1.1 Heart sounds:

As previously described at the previous chapter heart sound collected at normal and pathological cases were recorded and analyzed using fast Fourier Transform to get the frequency components of these signals.

5.1.1.1 Normal sound:

Normal heart sounds are generated by valve closure. Closures of the mitral and tricuspid valves produce S1 signal, while the closure of aortic and pulmonic valves produce S2 signal. Fig. 41 represents the apex auscultation of normal heart sounds in time domain, S1 is best hearing at the apex position. While fig. 42, 43 represents the aortic and pulmonic auscultation of normal heart sound, S2 is best hearing in these positions.
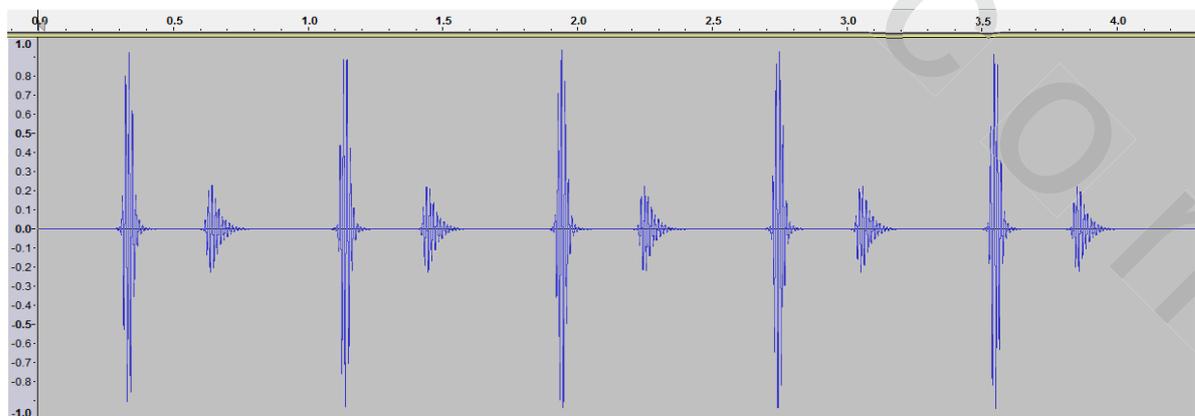
Fig. 41: Apex normal heart sound in time domain
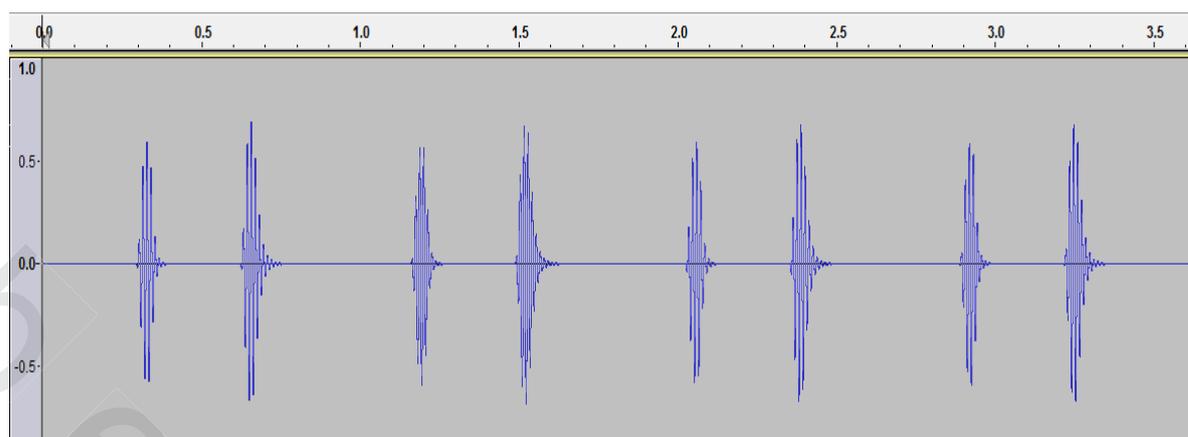
Fig. 42: Aortic normal in time domain
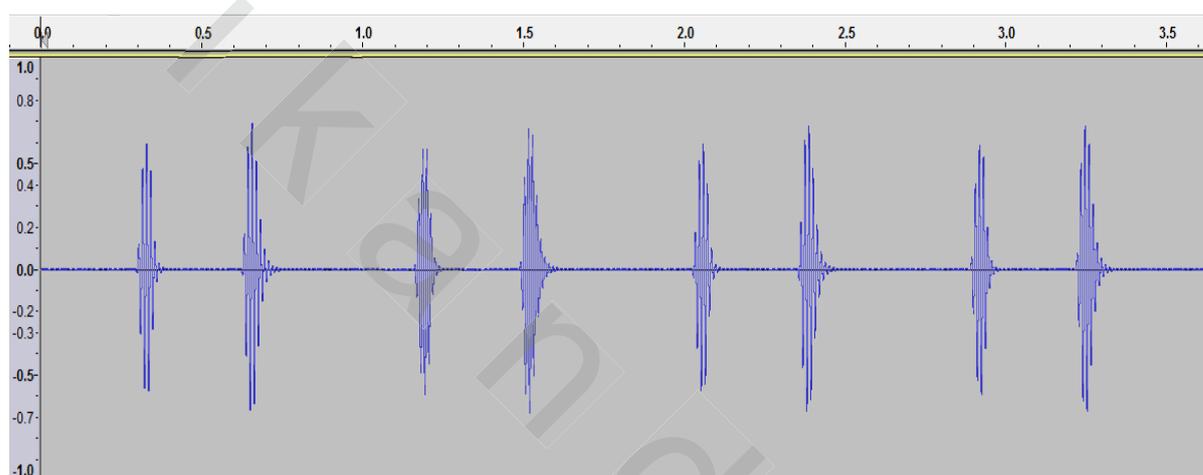
Fig. 43: Pulmonary normal in time domain

Fig. 44 represents the frequency spectrum of the normal apex position with amplitude of -17 dB, while fig. 45, 46 represents the frequency spectrum of normal aortic and pulmonic positions with amplitude of -10 dB.
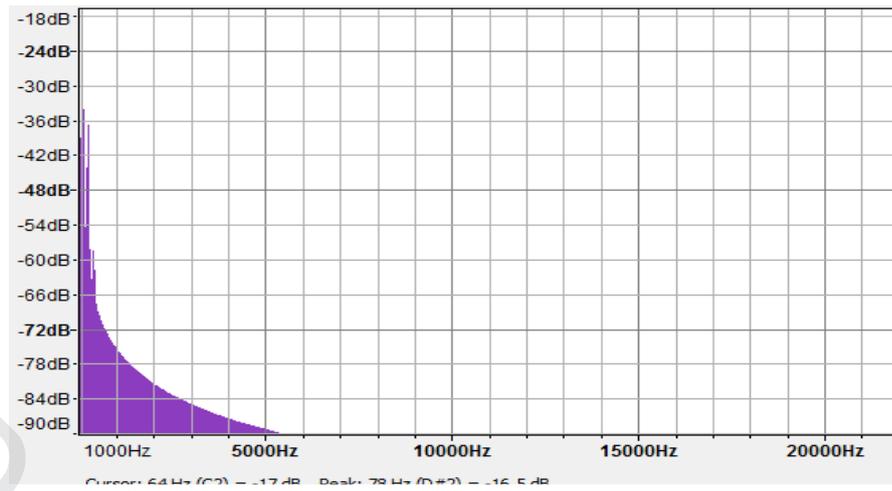
Fig. 44: The frequency domain of apex normal heart sound

Cursor: 64 Hz (C2) = -10 dB   Peak: 78 Hz (D#2) = -9.7 dB
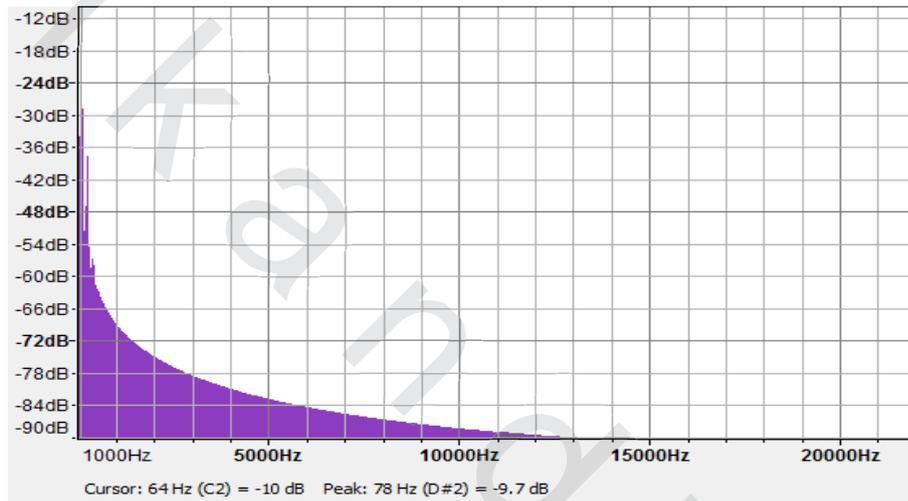
Fig. 45: The frequency domain of aortic normal

Cursor: 64 Hz (C2) = -10 dB   Peak: 78 Hz (D#2) = -9.7 dB
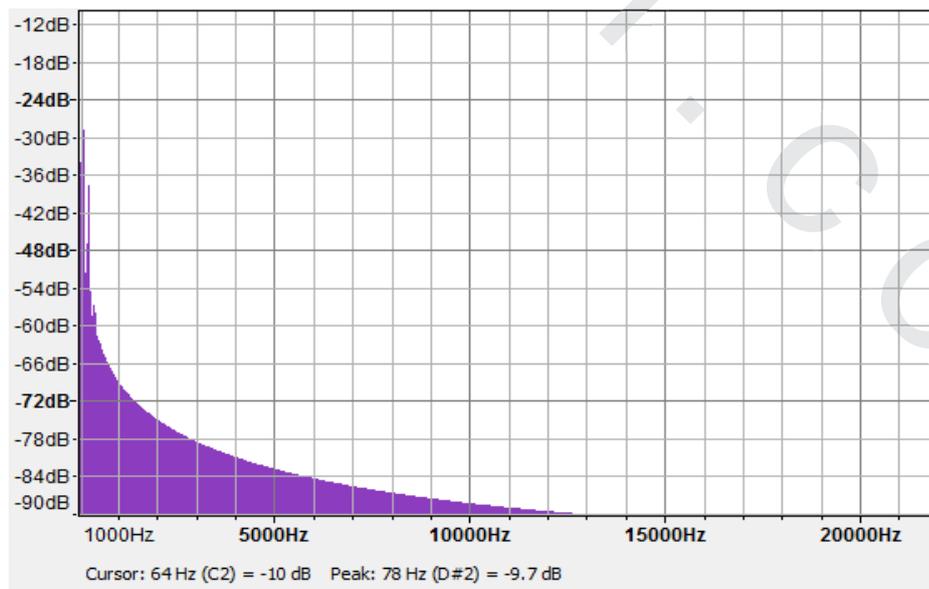
Fig. 46: The frequency domain of pulmonary normal

5.1.1.2 Abnormal heart sounds (S3, S4):

The S3 (Fig, 47) is a somewhat low-frequency sound in early diastole and is related to rapid filling of the ventricle. It is best heard at the apex at the left lateral decubitius position (LLD). It is commonly heard in normal children and young adults. A loud S3 is abnormal and is audible in conditions with dilated ventricles and decreased ventricular compliance.
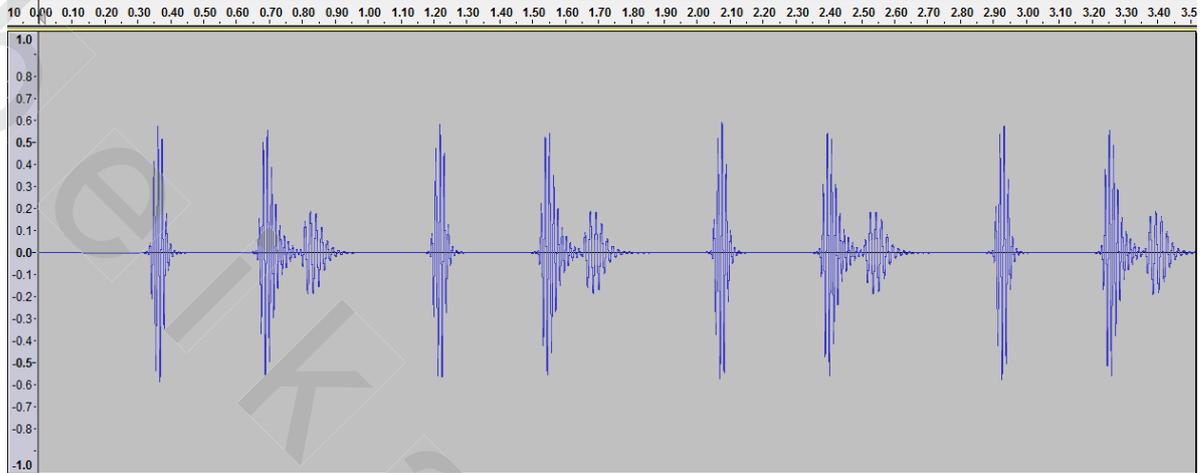
Fig. 47: Apex, S3 in time domain

The S4 (Fig. 48) appears at 0.04s after the P wave (late diastolic-just before S1), lasts 0.04-0.10s with low frequency sound. It is caused by the blood flow that hits the ventricular wall during the atrial systole, causing it to vibrate. It is physiological only in small children. If heard otherwise it is a sign of reduced ventricular compliance.
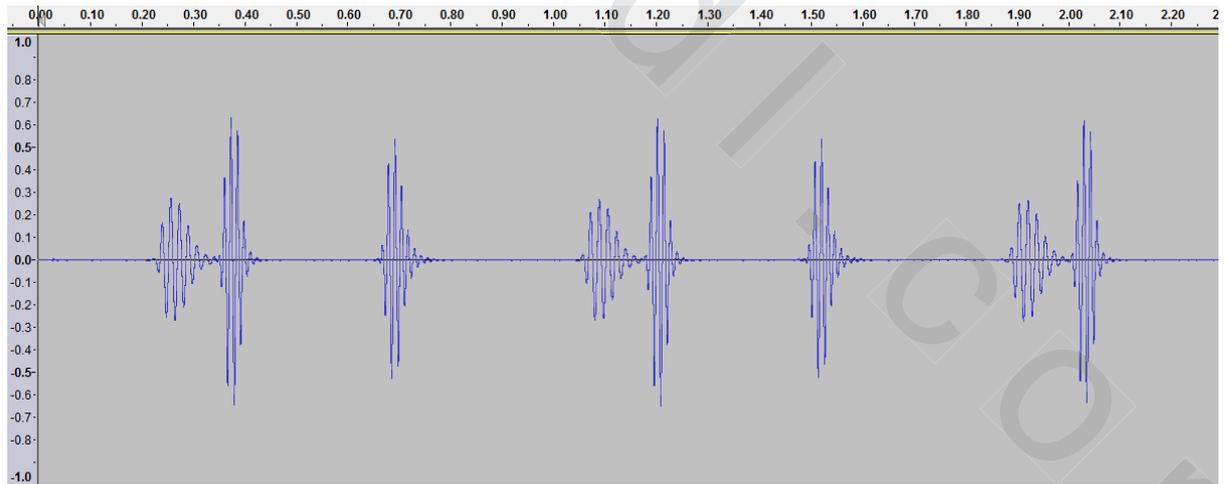
Fig. 48: Apex S4 in time domain

Figures 49-52 represent the frequency spectrum of normal and abnormal heart sounds S3 and S4 at the apex position with a peak frequency of 64 Hz and amplitude of -18 dB for both sounds.

Cursor: 64 Hz (C2) = -18 dB   Peak: 77 Hz (D#2) = -17.6 dB
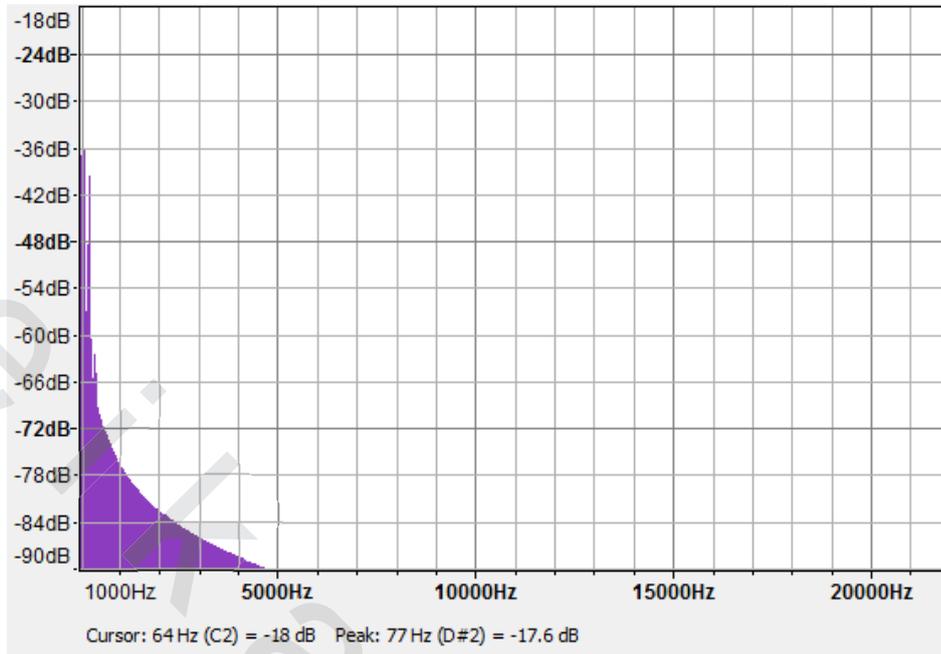
Fig. 49: The frequency domain of apex S3
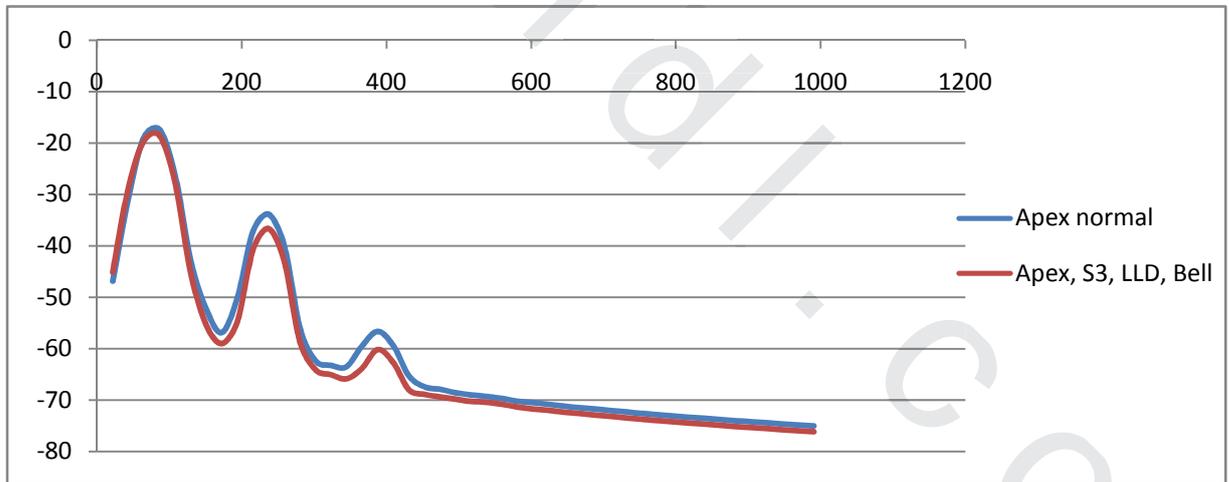
Fig. 50: Apex normal Vs apex S3

Cursor: 64 Hz (C2) = -18 dB   Peak: 77 Hz (D#2) = -17.9 dB
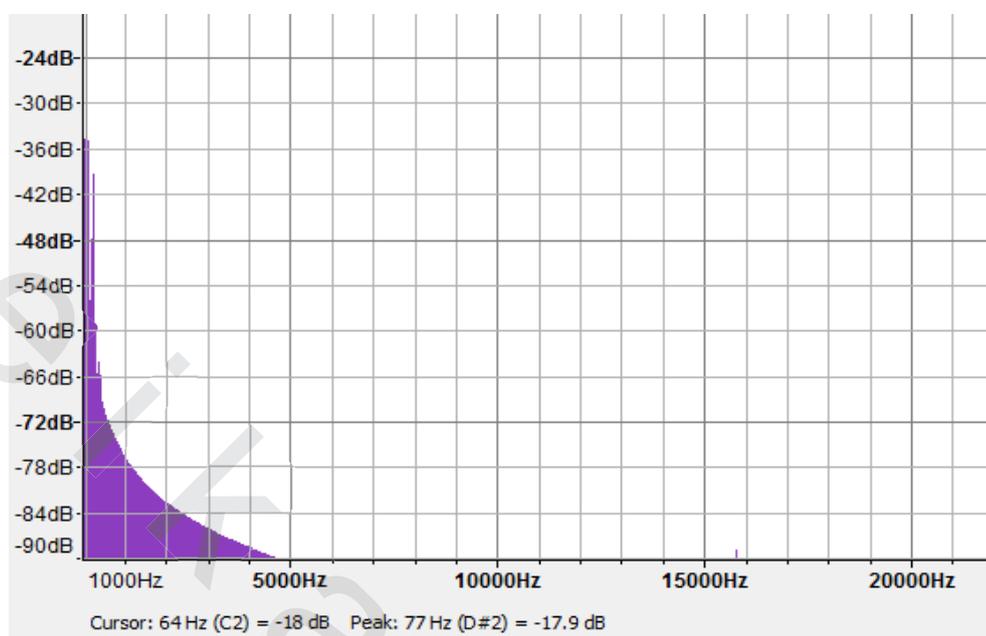
Fig. 51: The frequency domain of apex S4
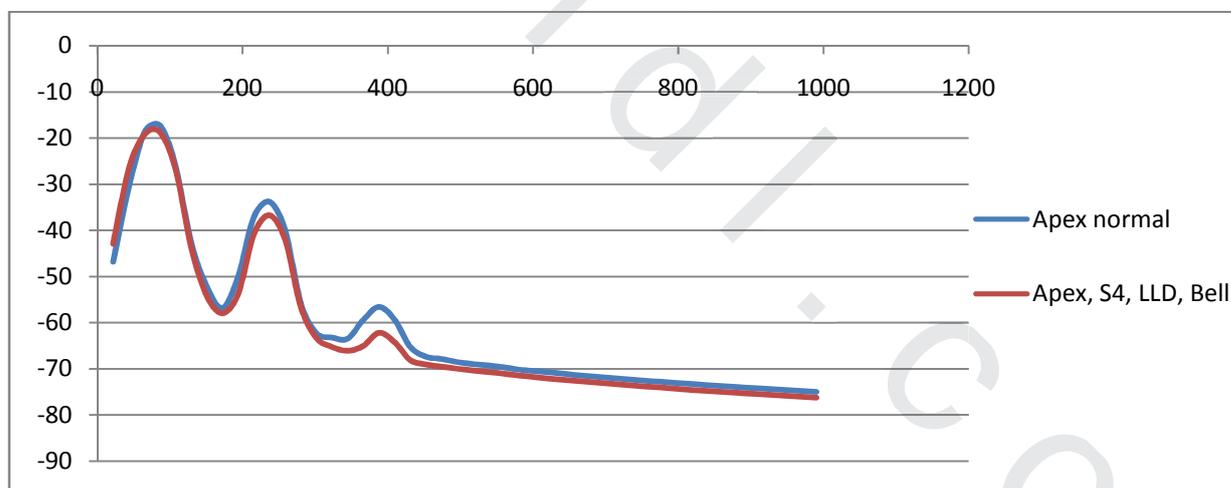
Fig. 52: Apex normal Vs apex S4

5.1.1.3 Abnormal heart sounds (Apex split S1, pulmonary split S2):

Split S1 (fig. 53) results from asynchronous closure of mitral (M1) and tricuspid (T1) valves. M1 is usually the earlier component, with T1 normally occurring ~20-30 ms after M1. Normal (if split is <30 ms apart); abnormal (if >60 ms).
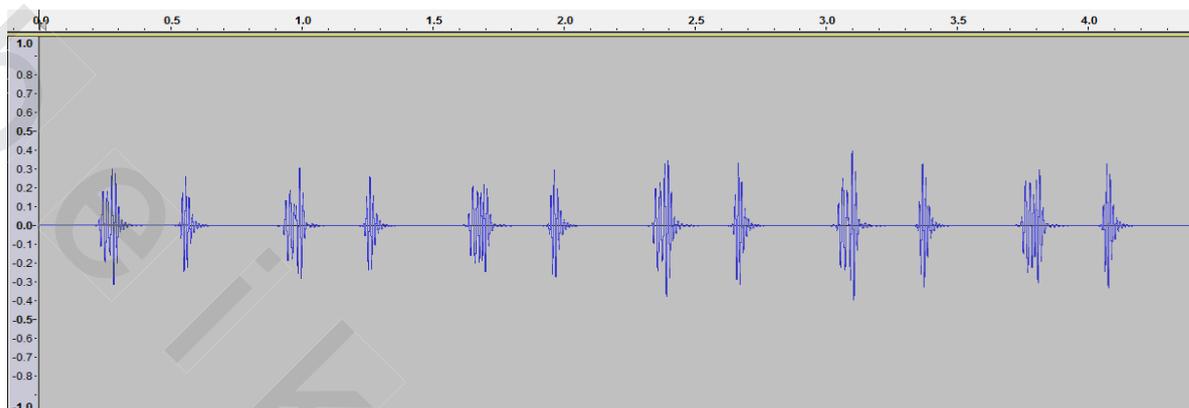
Fig. 53: Apex split S1 time domain

Fig. 54, 55 represents the frequency spectrum of abnormal heart sound split S1 with a frequency peak of 64 Hz and amplitude of -22 dB.

Cursor: 64 Hz (C2) = -22 dB   Peak: 73 Hz (D2) = -21.6 dB
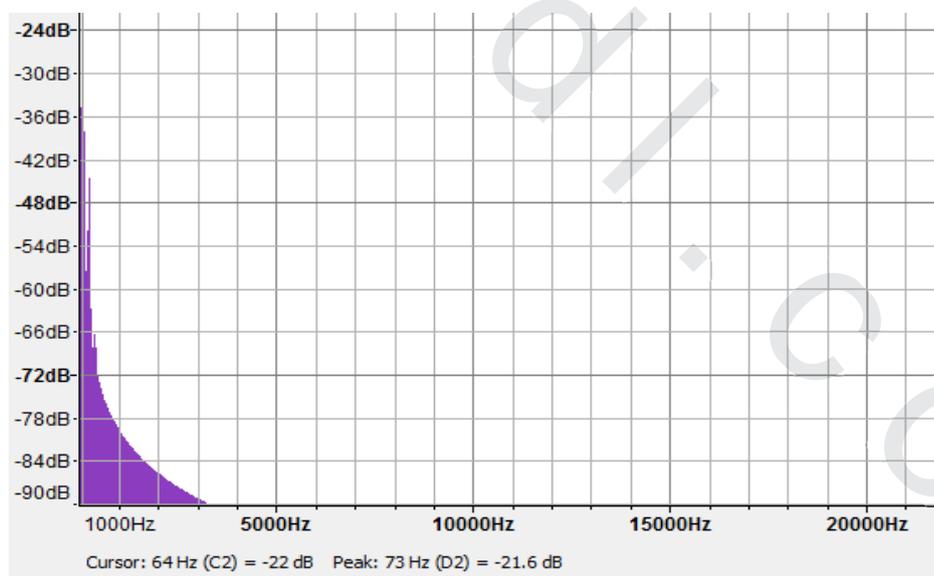
Fig. 54: The frequency domain of Split S1
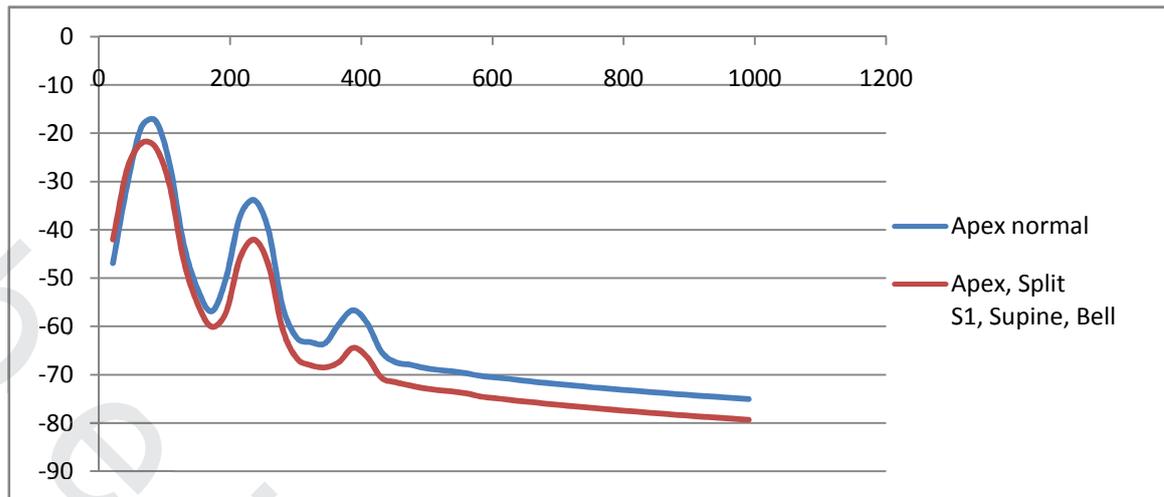
Fig. 55: Apex normal Vs Apex split S1

Persistent (audible) expiratory splitting (fig. 56) suggests an audible expiratory interval of at least 30 to 40 ms between the two sounds. Persistent splitting that is audible during both respiratory phases with appropriate inspirational and expirational directional changes may occur in the recumbent position in normal children, teenagers, and young adults. With the increased blood pressure within the right atrium and ventricle causes the pulmonary semilunar valve to close a fraction of a second later than the aortic semilunar valve, resulting in an audible split of the S2 sound shown at (fig. 57), with the first part of the split showing aortic valve closure and the second part of the split showing pulmonary valve closure.

Fig. 56: Pulmonary split S2 persistent
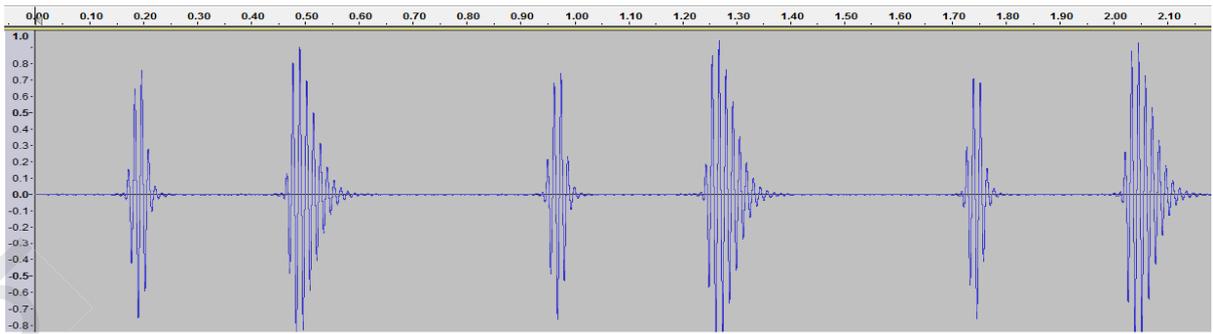
Fig. 57: Pulmonary split S2 transient

Figures 58- 61 represent the frequency spectrum of abnormal heart sounds split S2 persistent and split S2 transient with a frequency peak at 64 Hz and amplitude of -16 dB.
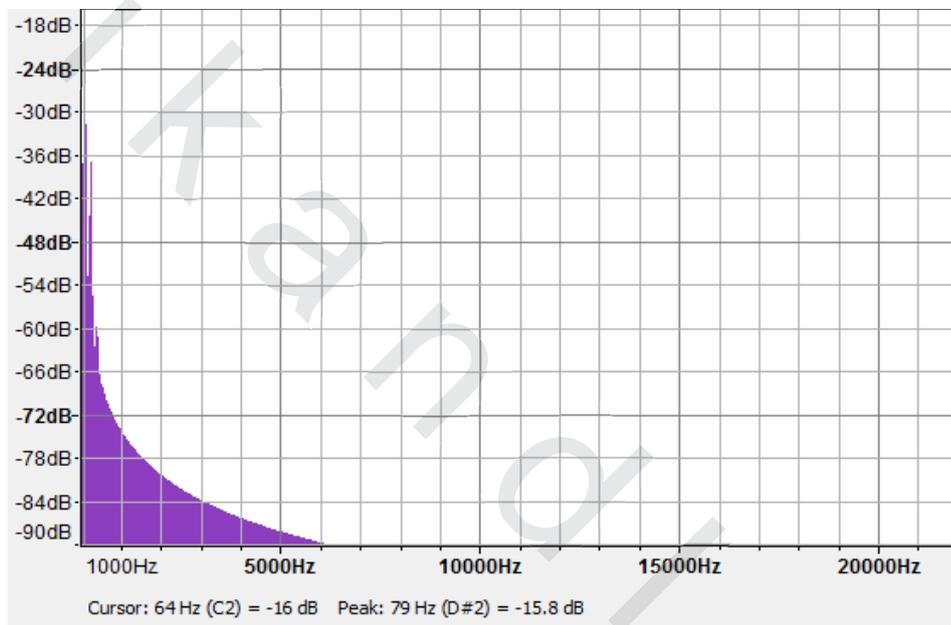
Fig. 58: The frequency domain of pulmonary split S2 persistent
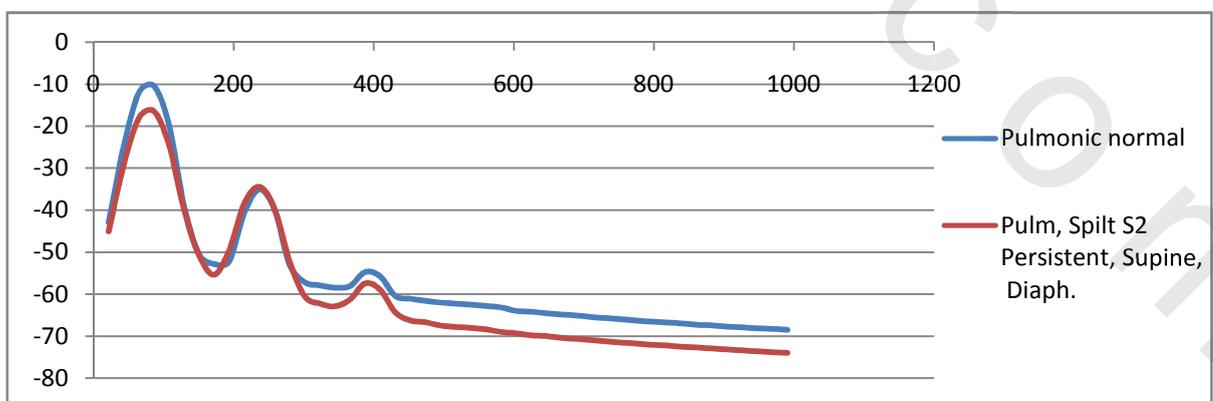
Fig. 59: Pulmonary normal Vs split S2 persistent
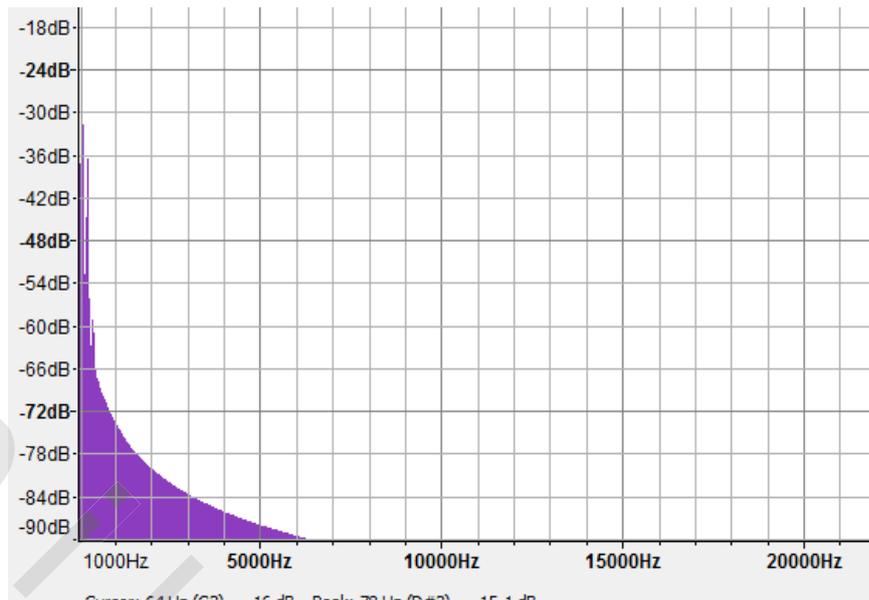
Fig. 60: The frequency domain of pulmonary split S2 transient
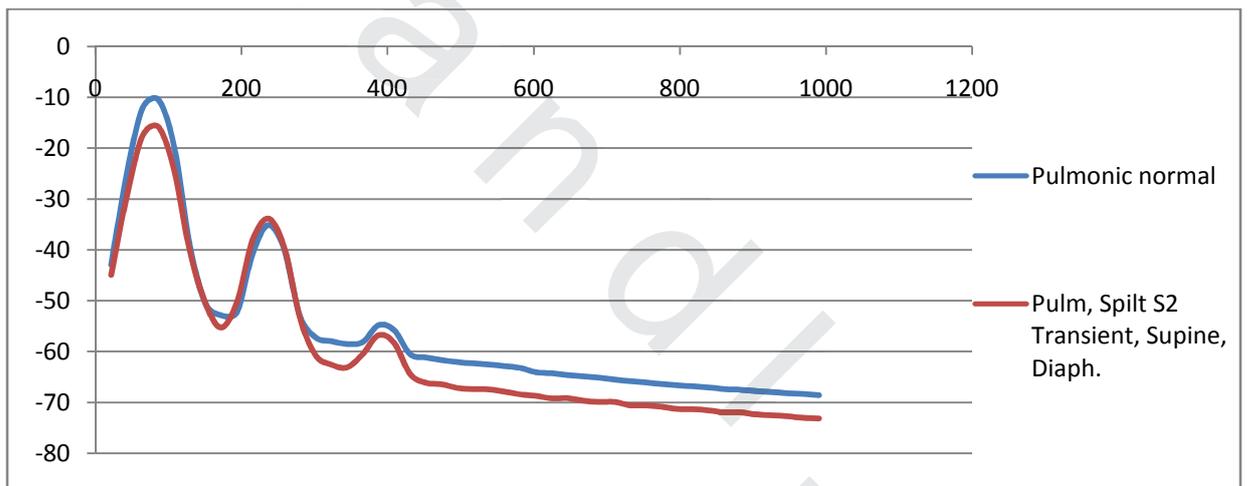
Fig. 61: Pulmonary normal Vs split S2 transient

5.1.1.4 Abnormal heart sound (Systolic murmur):

Early systolic murmurs (or short regurgitate murmurs) (fig. 62) begin with the S1, diminish in decrescendo, and end well before the S2, generally at or before midsystole. Only the three conditions that cause holosystolic murmurs (Ventricular Septal Defect (VSD), Mitral regurgitation (MR), and Tricuspid Regurgitation (TR)) are the causes of an early systolic murmur.
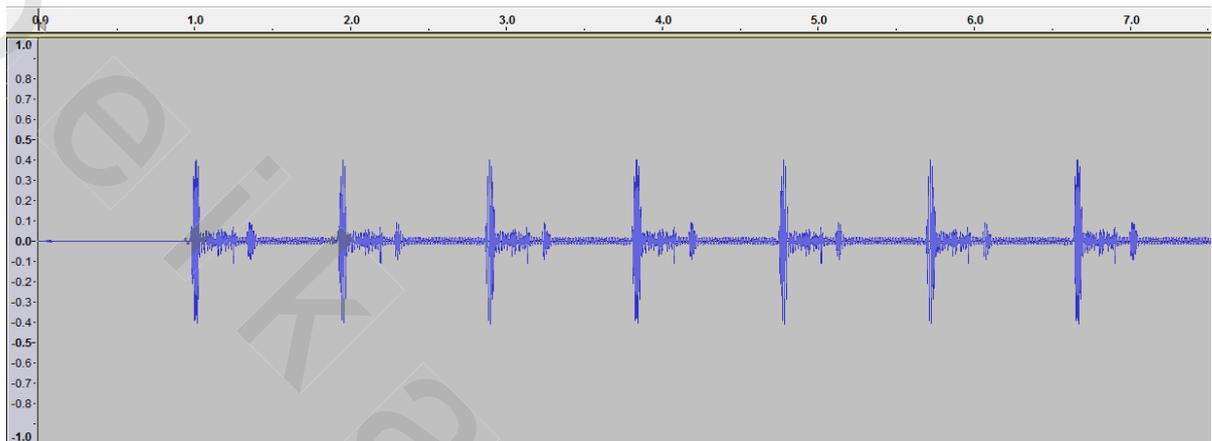
Fig. 62: Early systolic murmur in time domain

A midsystolic murmur (or ejection-type murmur) (fig. 63) begins after S1 and ends before S2. Midsystolic murmurs coincide with turbulent flow through the semilunar valves (e.g. aortic stenosis and pulmonic stenosis).

Fig. 63: Mid systolic murmur in time domain

The term late systolic (fig. 64) applies when a murmur begins in mid- to late systole and proceeds up to the S2. The late systolic murmur of Mitral Valve Prolapse (MVP) is prototypical.
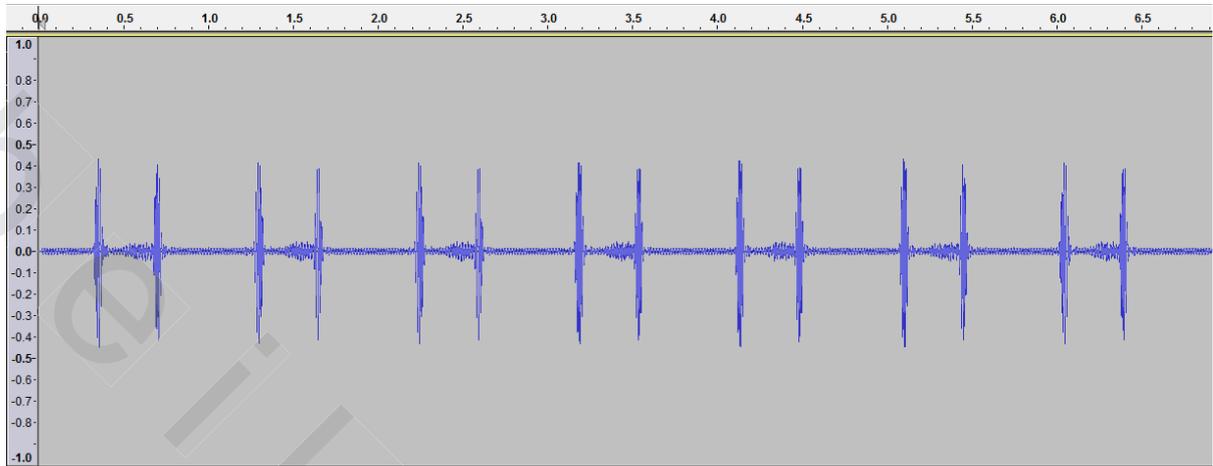
Fig. 64: Late systolic murmur in time domain

Holosystolic murmurs (fig. 65) begin with S1 and occupy all of systole up to the S2. No gap exists between the S1 and the onset of the murmur. These murmurs are associated with only the following three conditions: Ventricular Septal Defect (VSD), Mitral regurgitation (MR), and tricuspid regurgitation (TR).
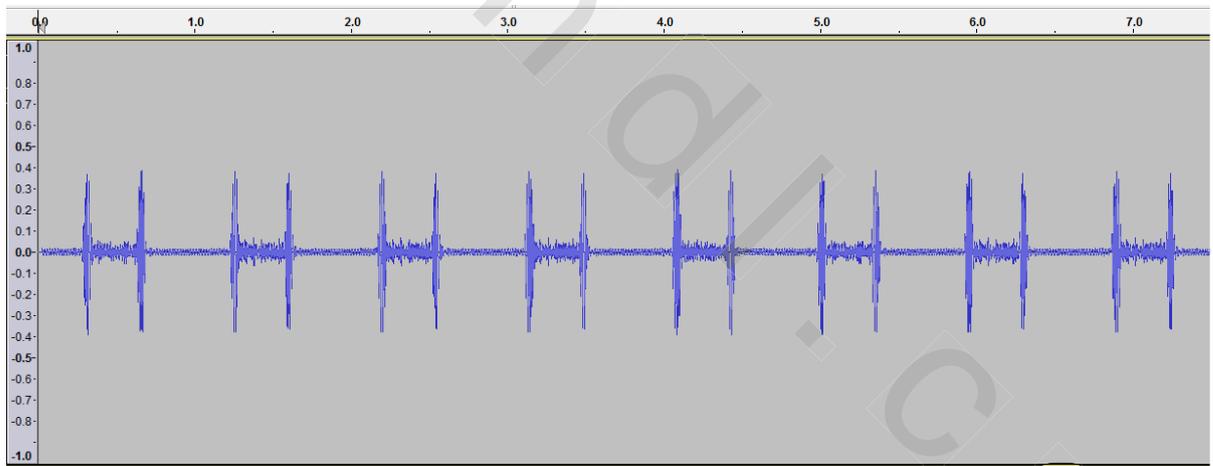
Fig. 65: Holo systolic murmur in time domain

Figures 66-73 represent the frequency spectrum of early systolic, mid systolic, late systolic, and holo systolic murmur respectively, with a frequency peak of 64 Hz, and amplitude ranging from -24 to -22.

Cursor: 64 Hz (C2) = -24 dB   Peak: 78 Hz (D#2) = -22.8 dB
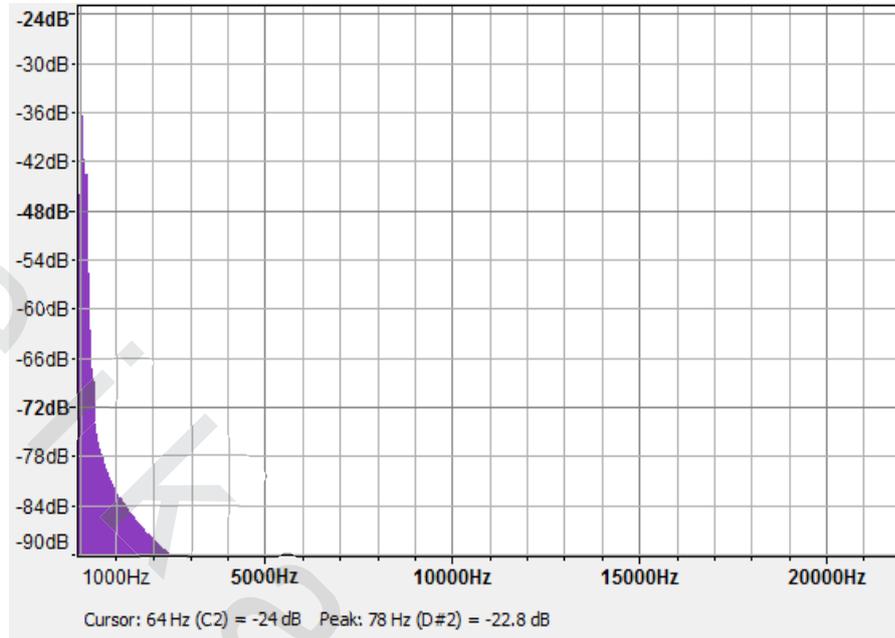
Fig. 66: The frequency domain of early systolic murmur
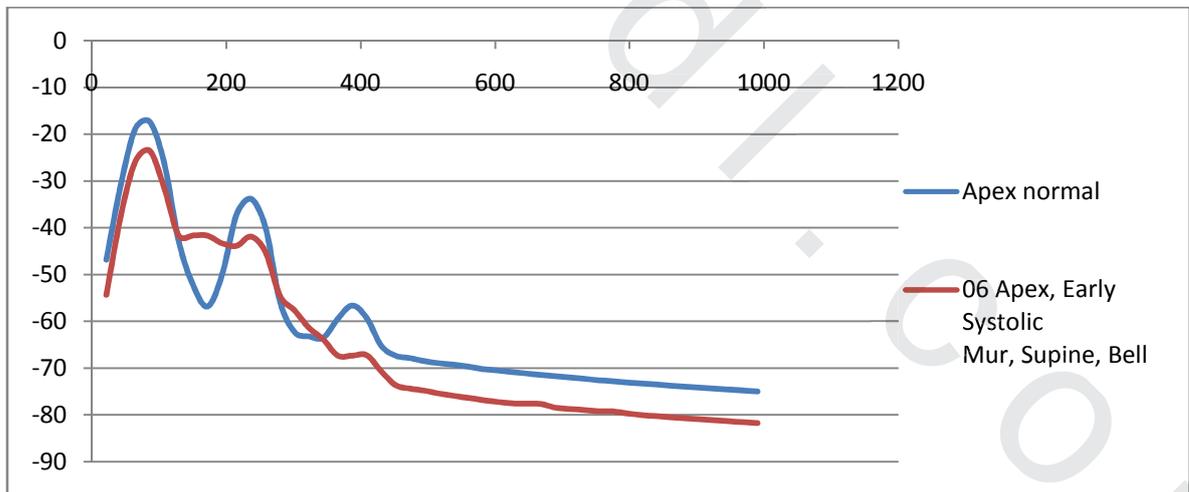
Fig. 67: Apex normal Vs early systolic murmur
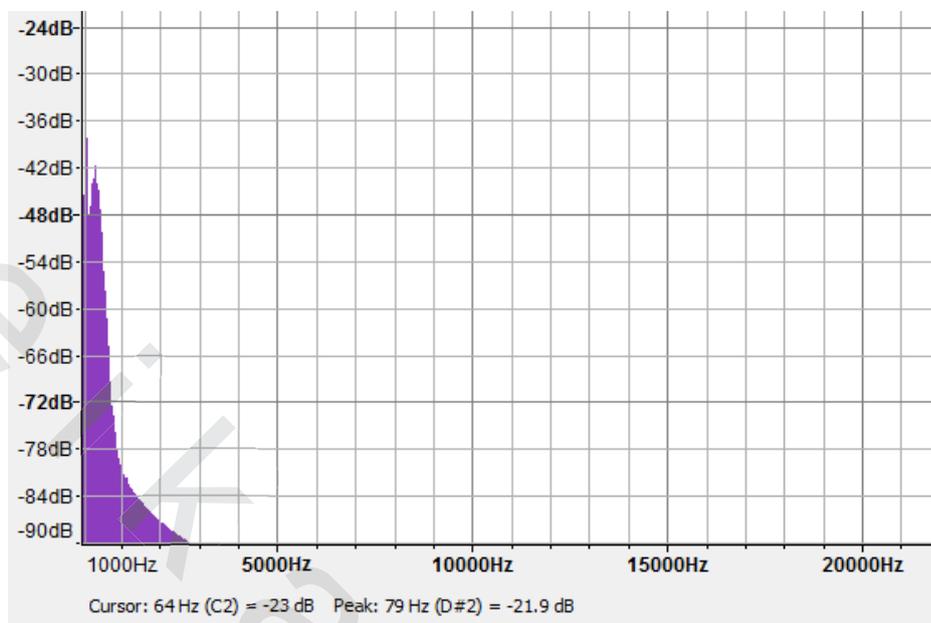
Fig. 68: The frequency domain of mid systolic murmur
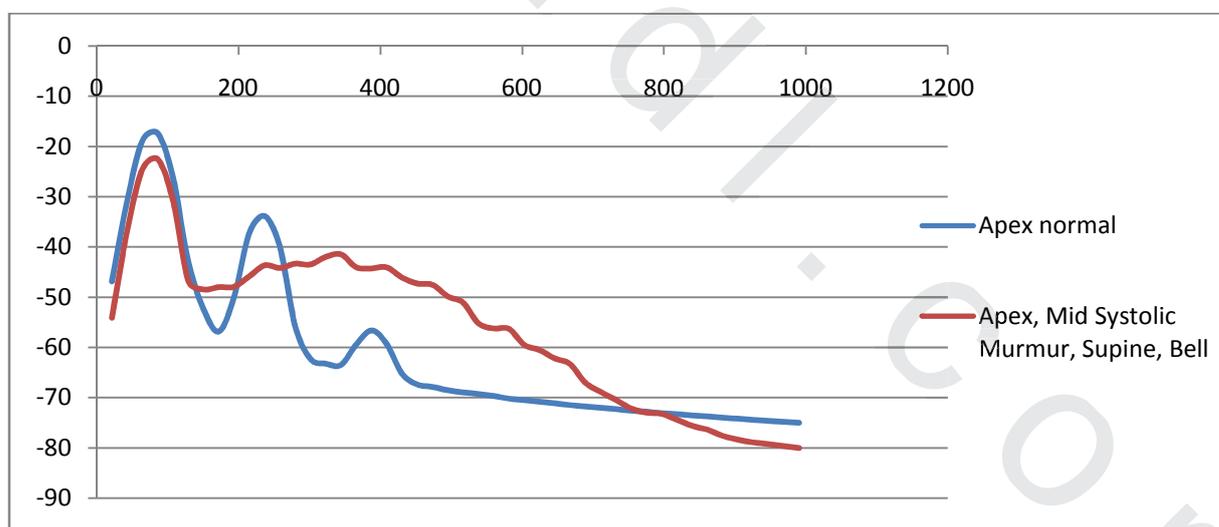
Fig. 69: Apex normal Vs mid systolic murmur

Cursor: 64 Hz (C2) = -22 dB   Peak: 79 Hz (D#2) = -21.1 dB
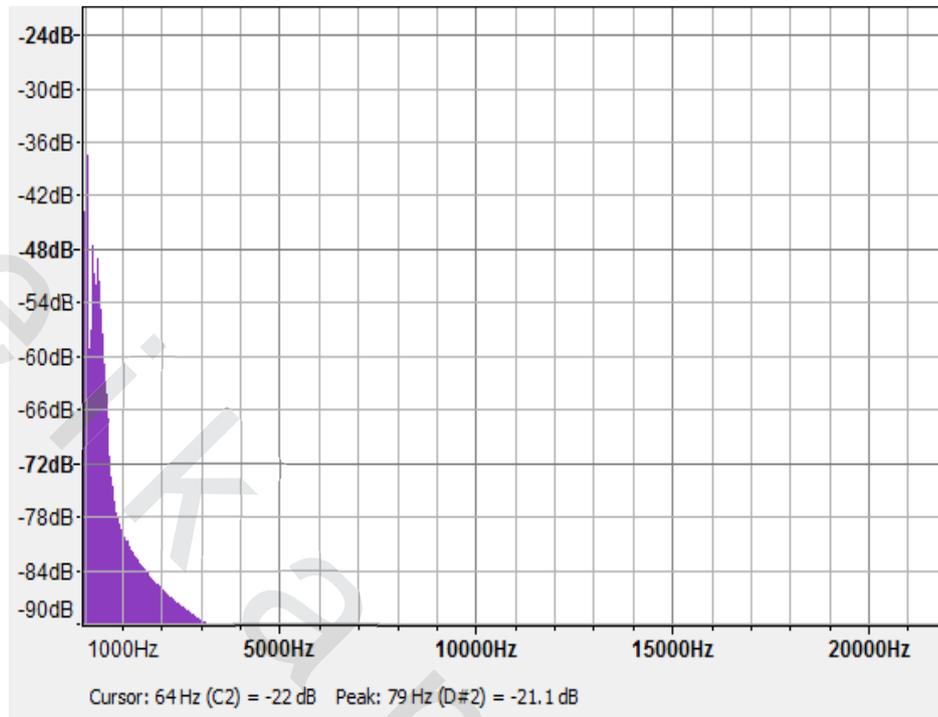
Fig. 70: The frequency domain of late systolic murmur
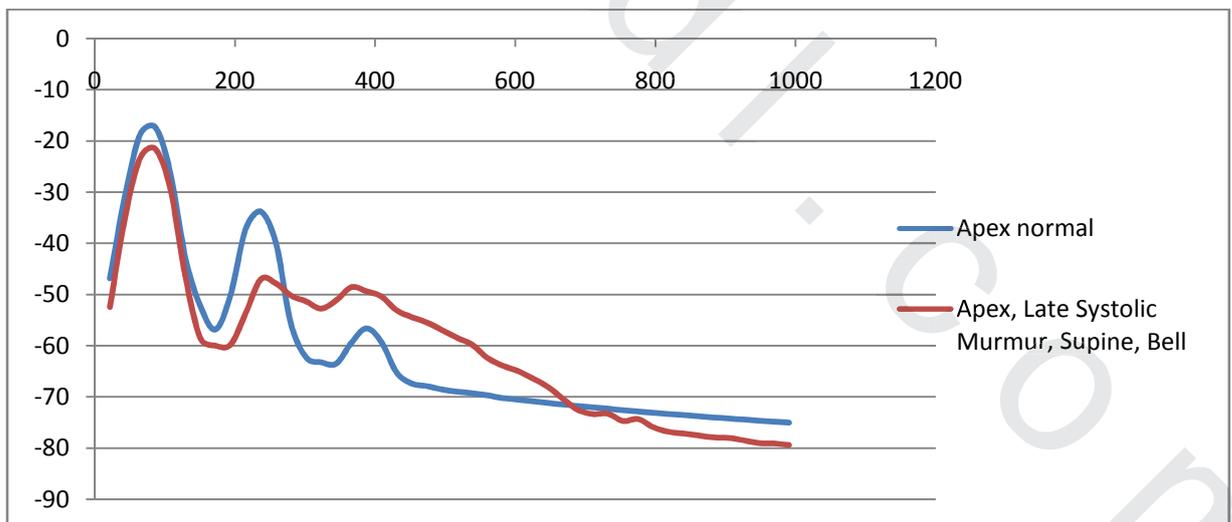
Fig. 71: apex normal Vs late systolic murmur

Cursor: 64 Hz (C2) = -22 dB   Peak: 80 Hz (D#2) = -21.3 dB
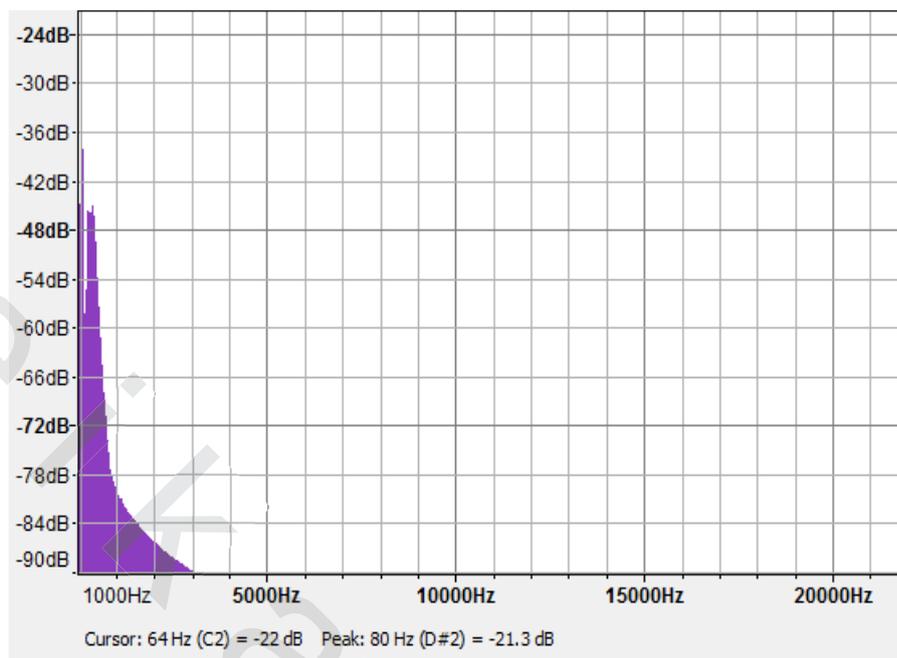
Fig. 72: The frequency domain of holo systolic murmur
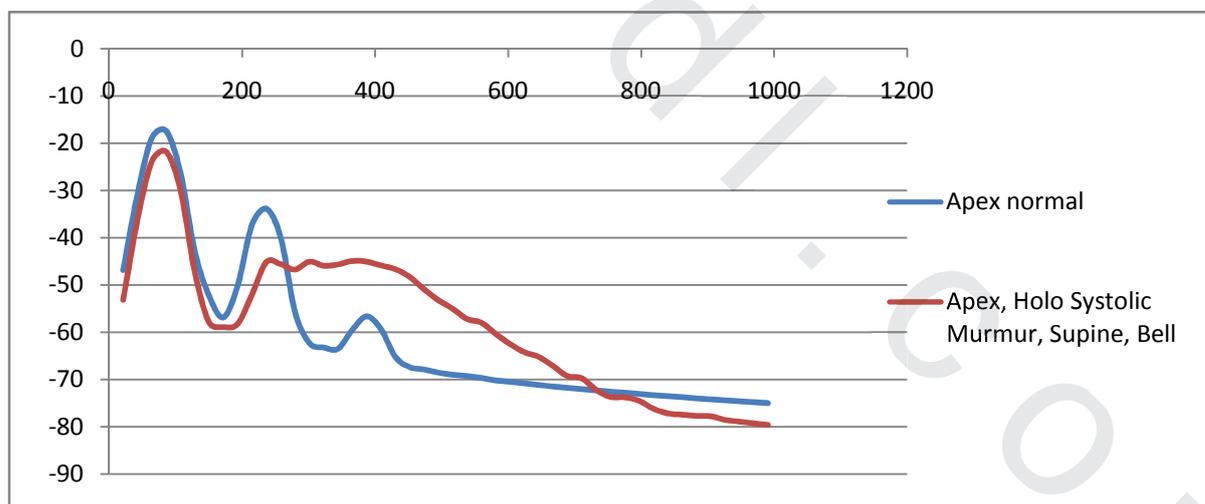
Fig. 73: Apex normal Vs holo systolic murmur

5.1.1.5 Abnormal heart sounds (diastolic murmur):

Early diastolic Murmur (EDM) (fig. 74) is a high-frequency and (usually) decrescendo murmur that begins with S2 and results from aortic or pulmonic valve backflow (Aortic regurgitation).
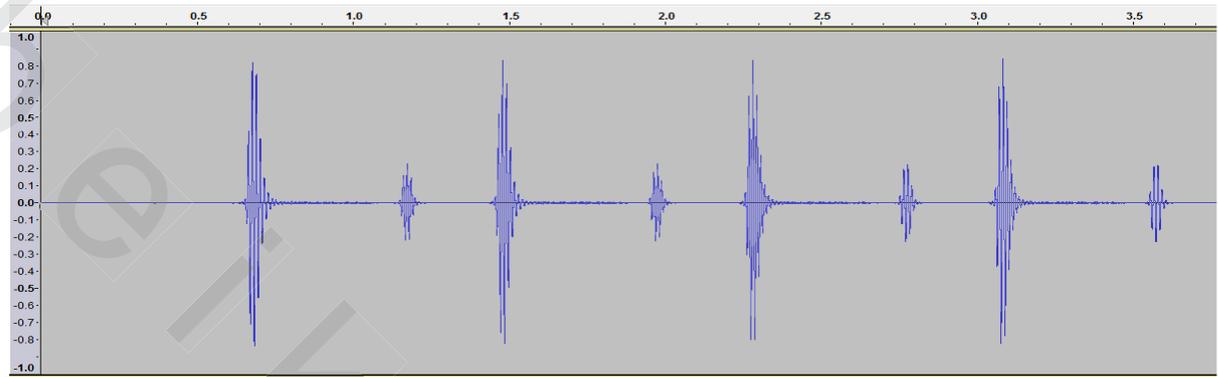
Fig. 74: Early diastolic murmur in time domain

Figures 75, 76 represent the frequency spectrum of early diastolic murmur, with a frequency peak of 64 Hz, and amplitude of -18.

Cursor: 64 Hz (C2) = -18 dB   Peak: 79 Hz (D#2) = -17.5 dB
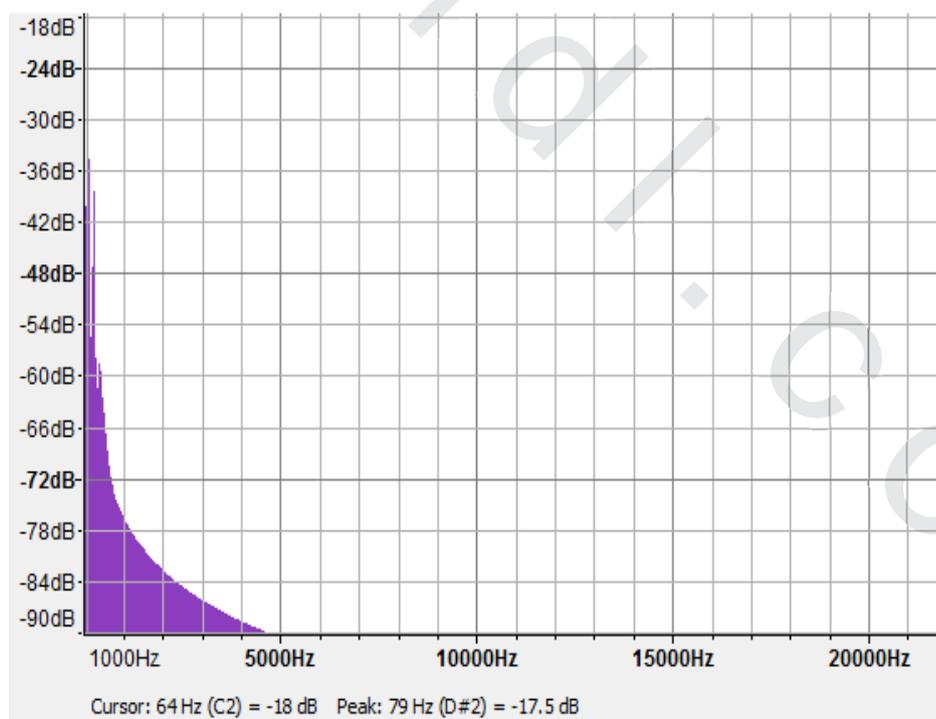
Fig. 75: The frequency domain of early diastolic murmur
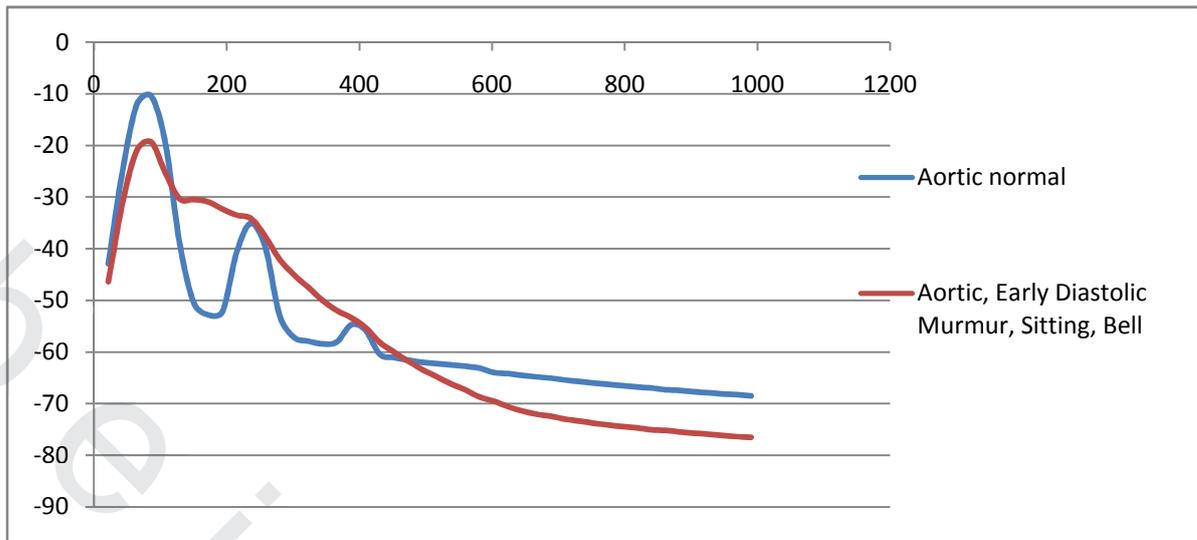
Fig. 76: aortic normal Vs early diastolic murmur

5.1.1.6 Abnormal heart sound (opening snap):

There is an opening snap 50 milliseconds into diastole (fig. 77). As mitral stenosis becomes more severe the opening snap will occur earlier in diastole. The opening snap is followed by a low frequency murmur which occupies the remainder of diastole.
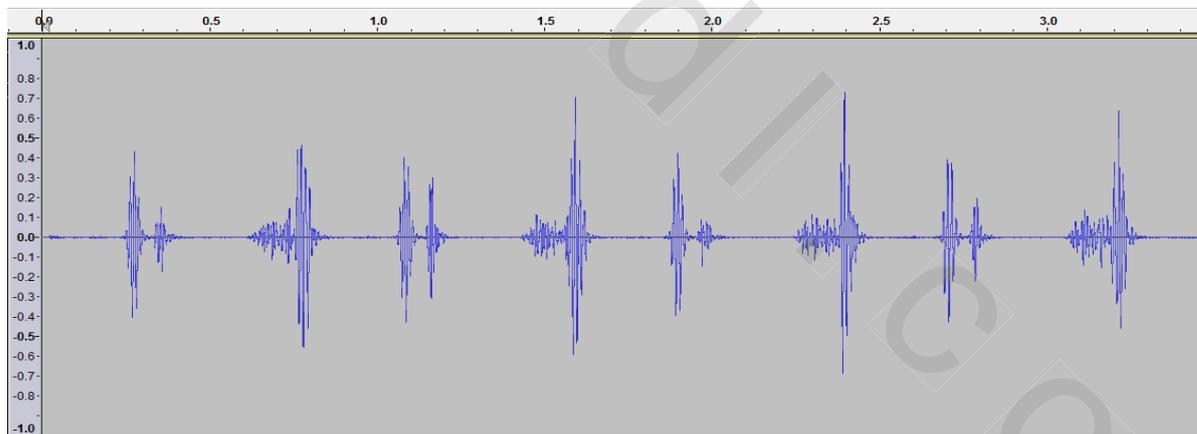
Fig. 77: Opening snap in time domain

Figures 78, 79 represent the frequency spectrum of opening snap, with a frequency peak of 64 Hz, and amplitude of -21.
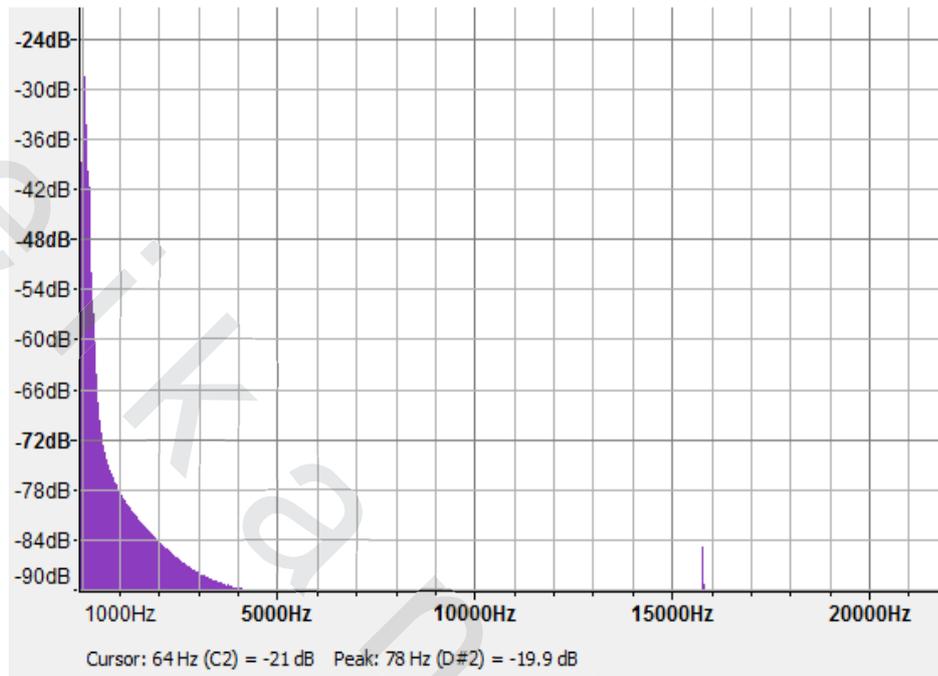
Fig. 78: The frequency domain of opening snap
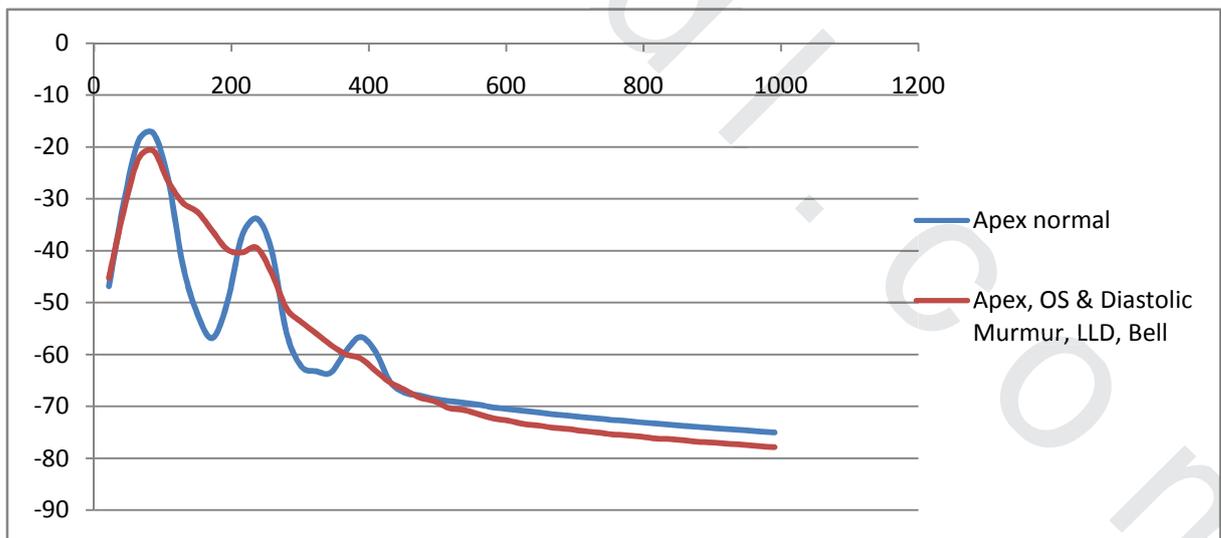
Fig. 79: Apex normal Vs opening snap

5.1.2 Lung sound analysis:

There are many sounds produced within the body due to various internal organs such as the heart and lungs. Sounds emitted from the lungs are referred to as breath sounds. Breath sounds signals were recorded for normal and abnormal cases using the digital oscilloscope in the time and frequency domain and Fast Fourier transform was calculated using MATLAB computer program.

5.1.2.1 Normal lung sound:

The sound of normal breathing heard over the surface of the chest is markedly influenced by the anatomical structures between the site of sound generation and the site of auscultation. Characteristically, normal lung sounds are heard clearly during inspiration but only in the early phase of expiration (fig. 80).
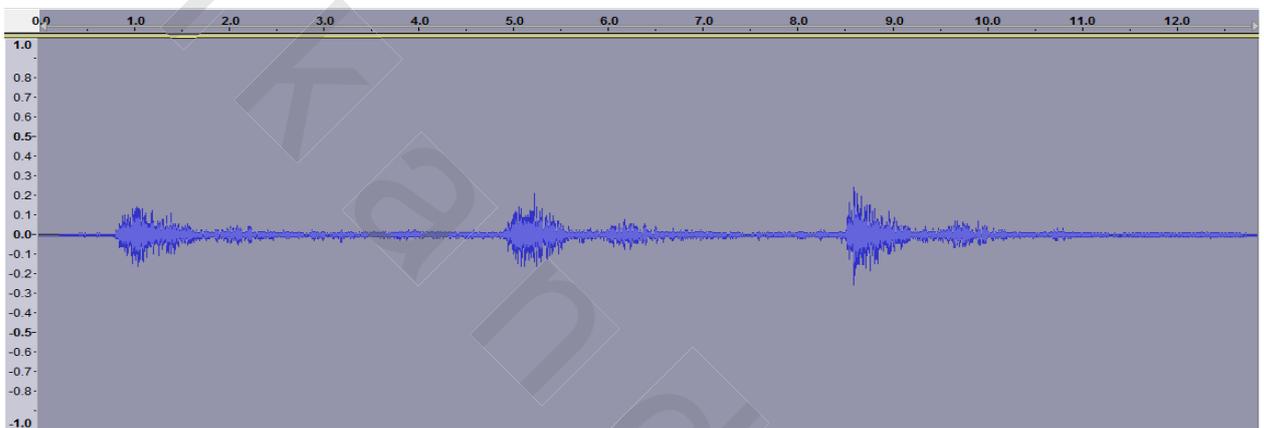
Fig. 80: Normal vesicular lung sound in time domain
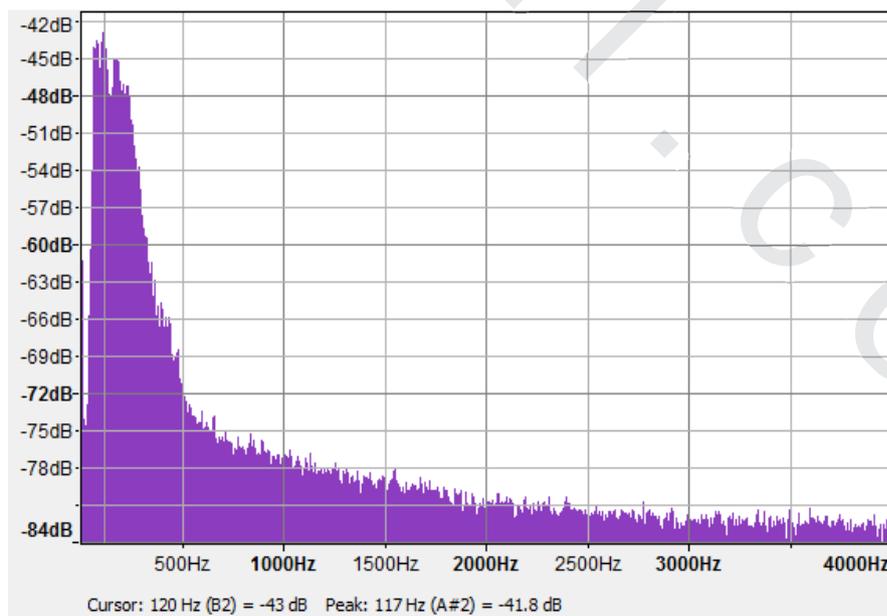
Fig. 81: The frequency domain of normal vesicular lung sounds

Figures 81, 82 shows the frequency range of normal lung sounds appears to be narrower than that of tracheal sounds, extending from below 100 Hz to 1000 Hz, with a sharp drop at approximately 100 to 200 Hz.
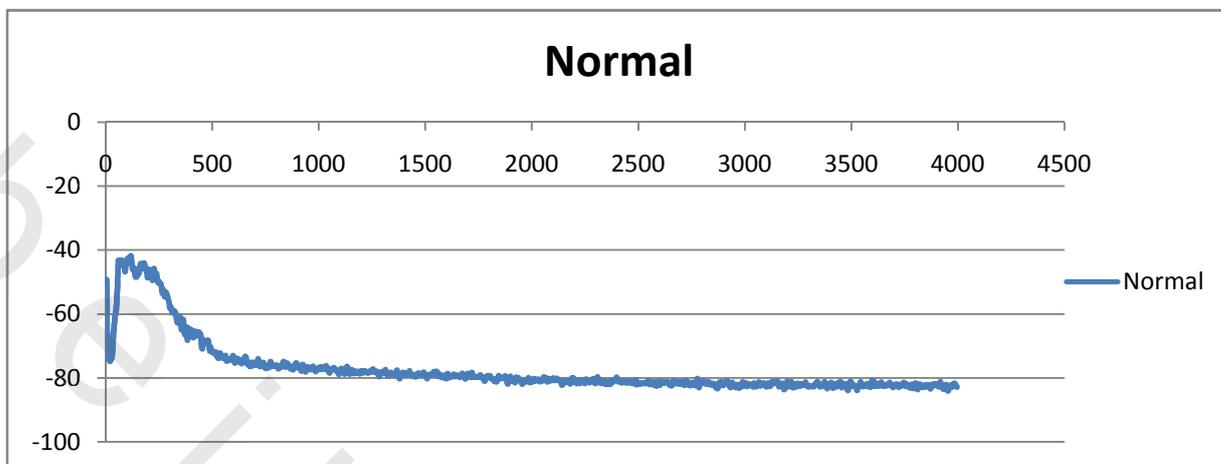
Fig. 82: The frequency peak of normal vesicular lung sound

5.1.2.2 Abnormal lung sounds (Coarse crackles):

Coarse crackles (figures 83- 85) are probably produced by boluses of gas passing through airways as they open and close intermittently. Coarse crackles are commonly heard in patients with obstructive lung diseases, including COPD, bronchiectasis, and asthma, usually in association with wheezes. They are also often heard in patients with pneumonia and those with congestive heart failure. Typical frequency about 350 Hz. Typical duration about 15 ms.
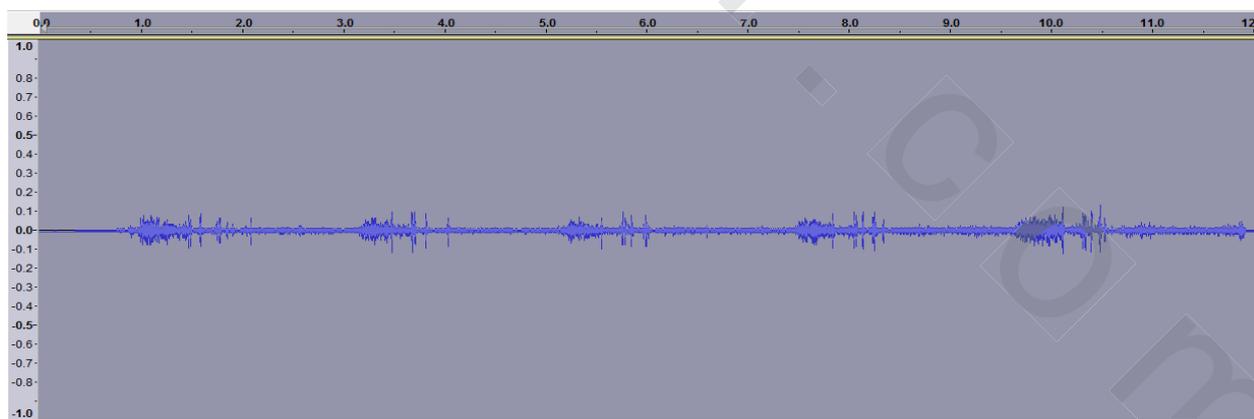
Fig. 83: Coarse crackles in time domain
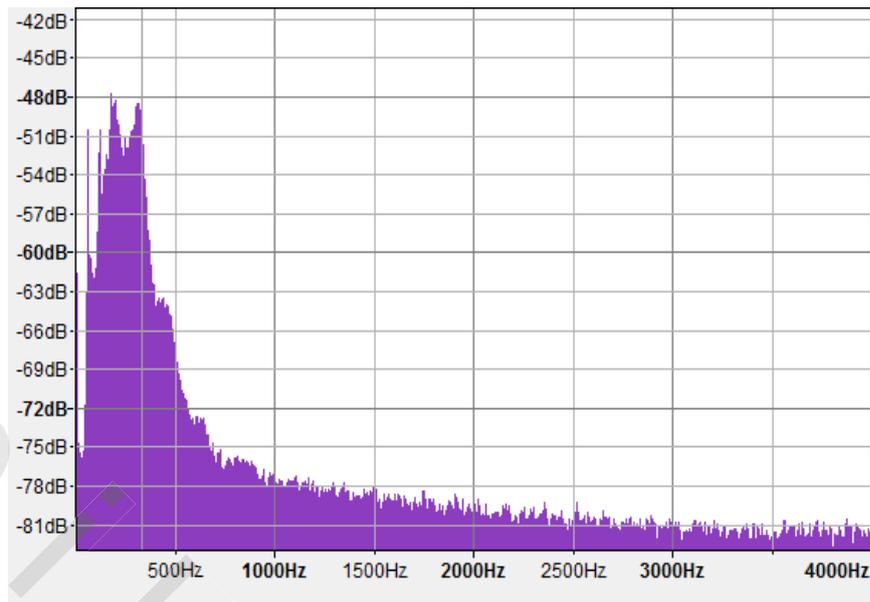
Fig. 84: The frequency domain of coarse crackles
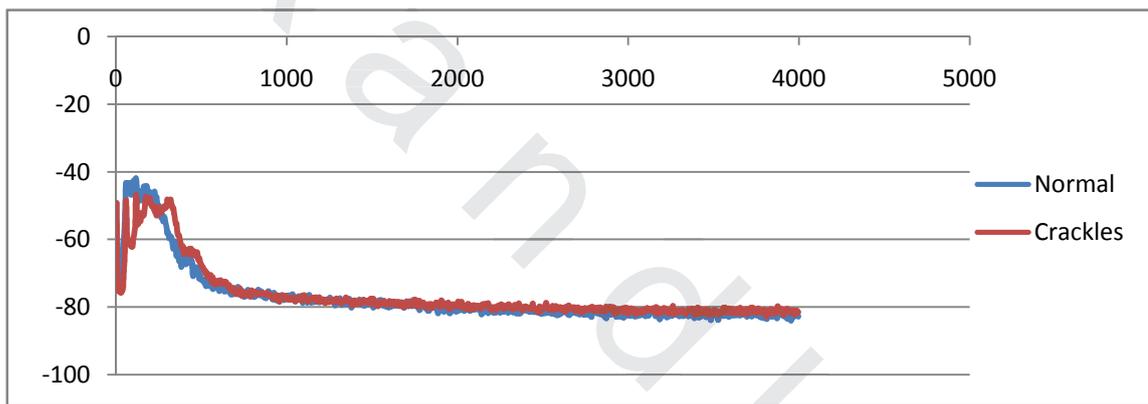
Fig. 85: Normal sound Vs Coarse crackles

5.1.2.3 Inspiratory stridor:

It is characterized by regular, sinusoidal oscillations with a peak frequency of approximately 275 Hz (figures 86- 88). In cases of such obstruction, stridor can be distinguished from wheeze because it is more clearly heard on inspiration than on expiration and is more prominent over the neck than over the chest. Although stridor is usually inspiratory, it can also be expiratory or biphasic.
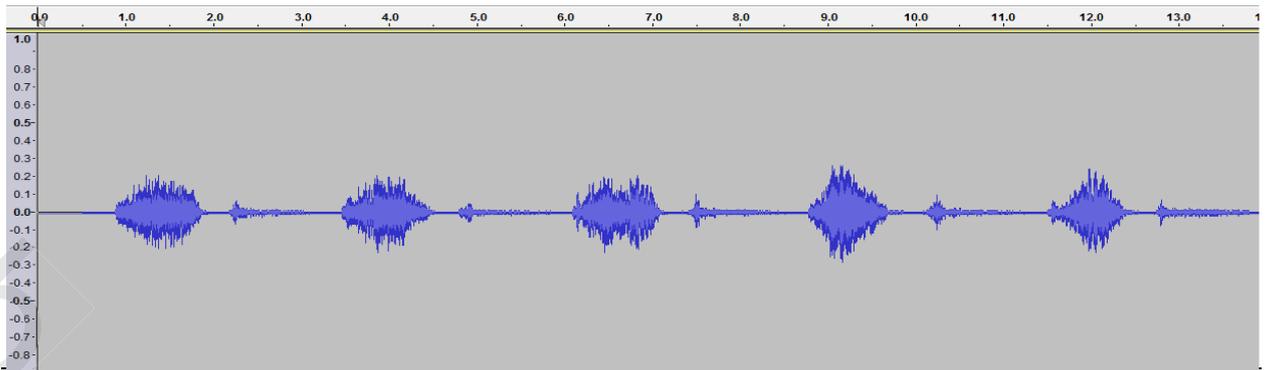
Fig. 86: Inspiratory stridor in time domain

Cursor: 275 Hz (C#4) = -35 dB   Peak: 278 Hz (C#4) = -35.7 dB
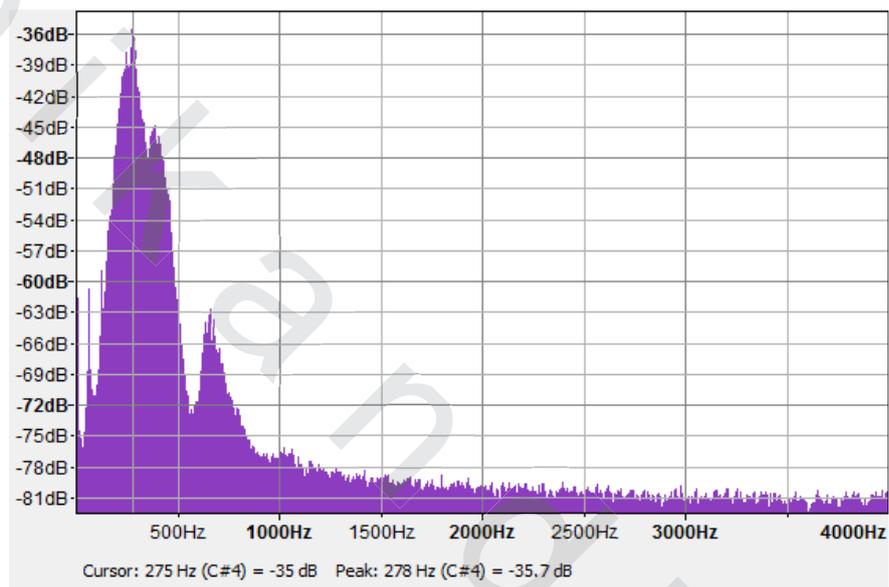
Fig. 87: The frequency domain of inspiratory stridor
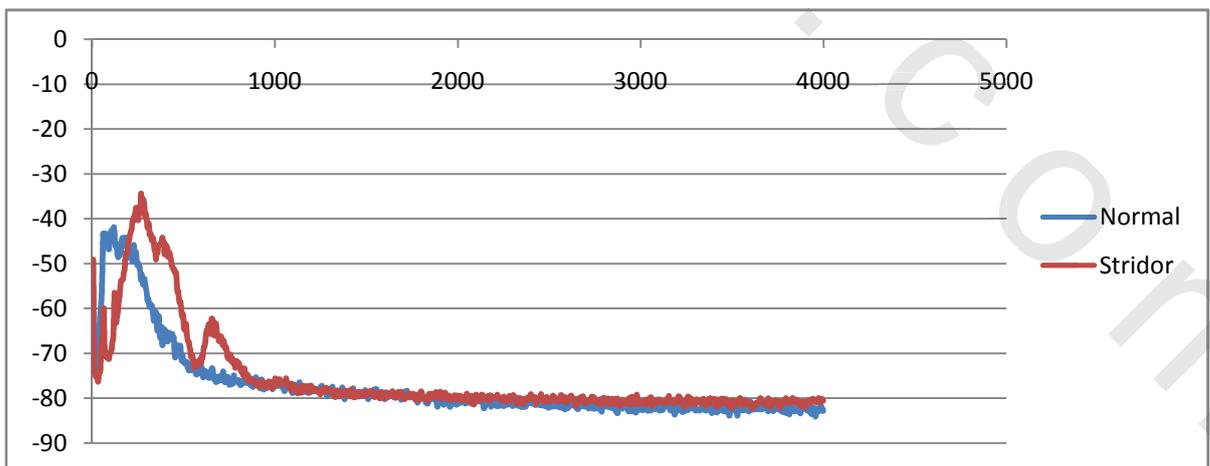
Fig. 88: Normal lung sound Vs inspiratory stridor

5.1.2.4 Pleural friction:

The pleural friction (figures 89- 91) rub is biphasic, with the expiratory sequence of sounds mirroring the inspiratory sequence. The waveform is similar to that seen with crackles, except for its longer duration and lower frequency. Typical frequency of <350 Hz, and duration of >15 ms.
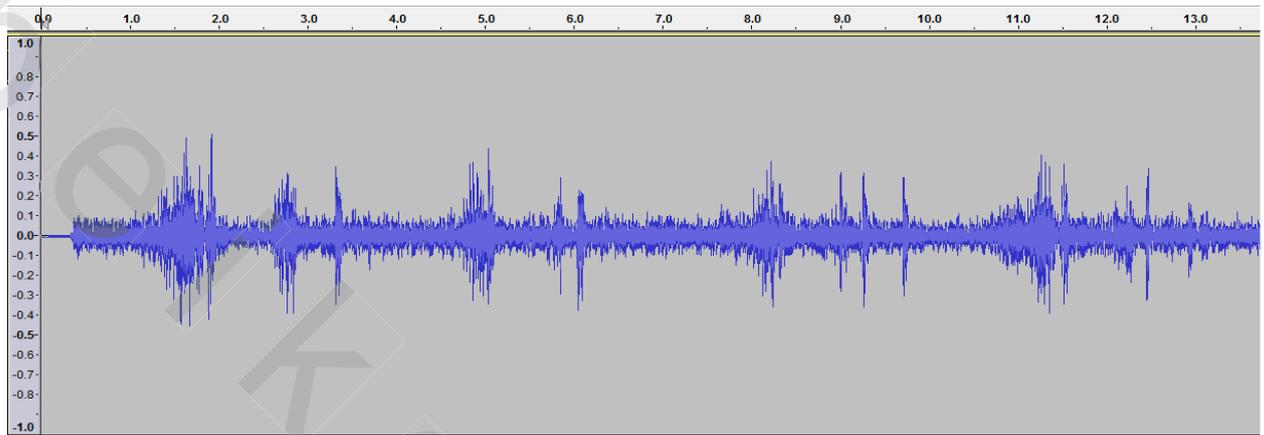
Fig. 89: Pleural friction in time domain
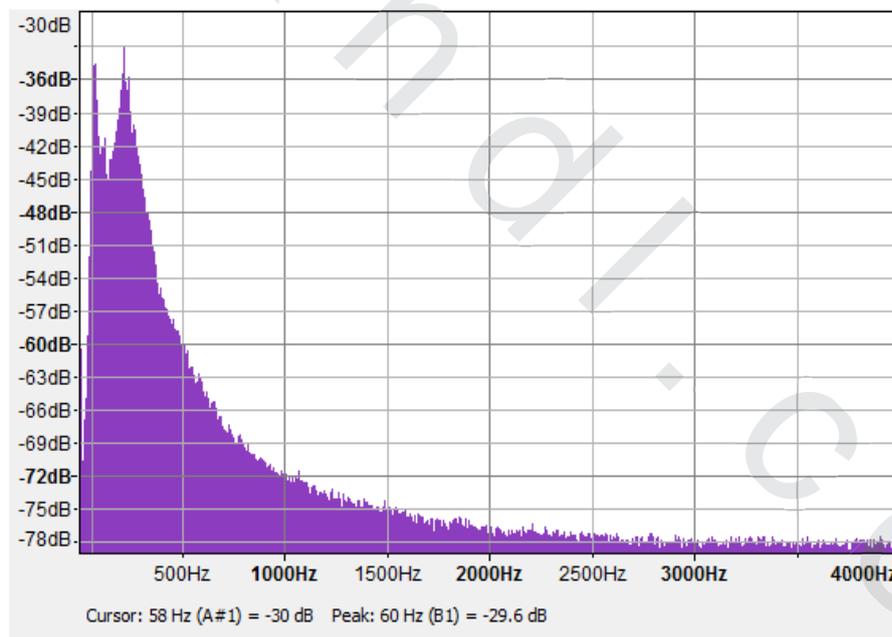
Fig. 90: The frequency domain of pleural friction
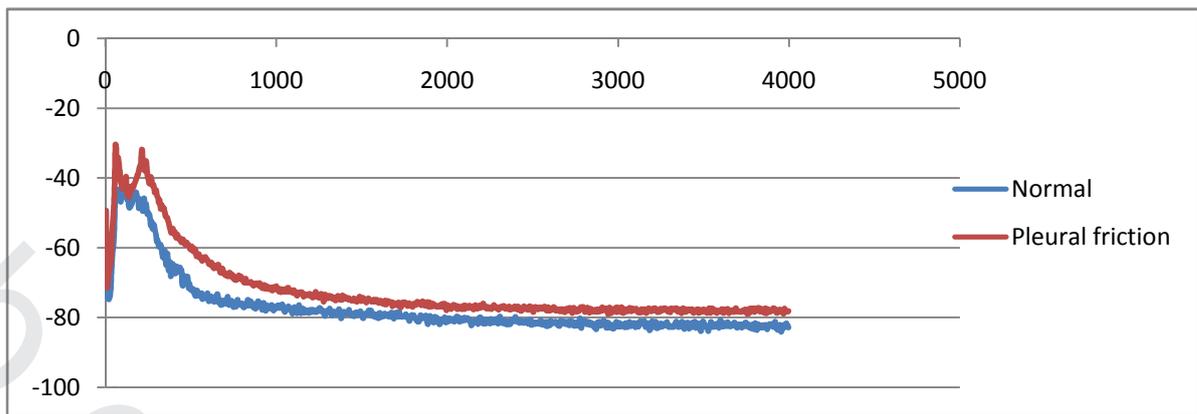
Fig. 91: Normal lung sound Vs pleural friction

5.1.2.5 Wheezing:

Wheezes can be inspiratory, expiratory, or biphasic (figures 92- 94). Although typically present in obstructive airway diseases, especially asthma, they are not pathognomonic of any particular disease. In asthma and COPD, wheezes can be heard all over the chest, making their number difficult to estimate. Localized wheeze is often related to a local phenomenon, usually an obstruction by a foreign body, mucous plug, or tumor.
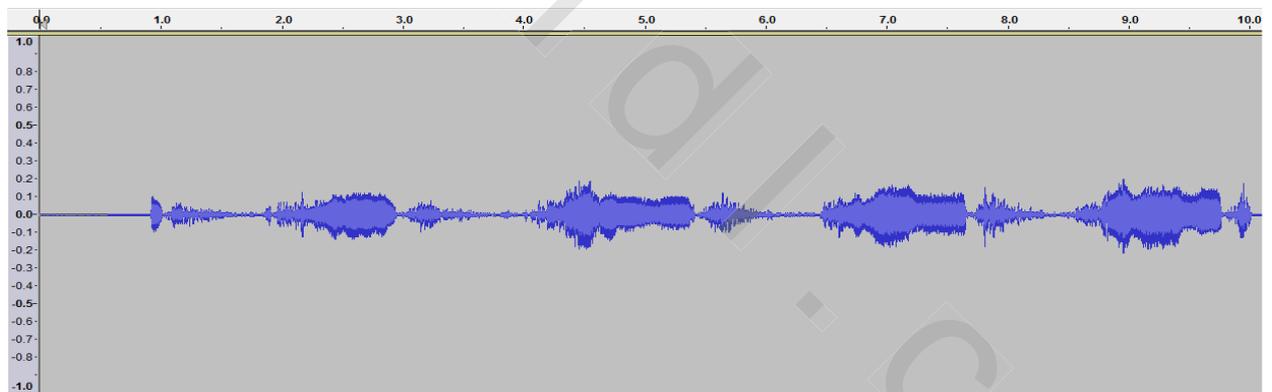
Fig. 92: Wheezing in time domain
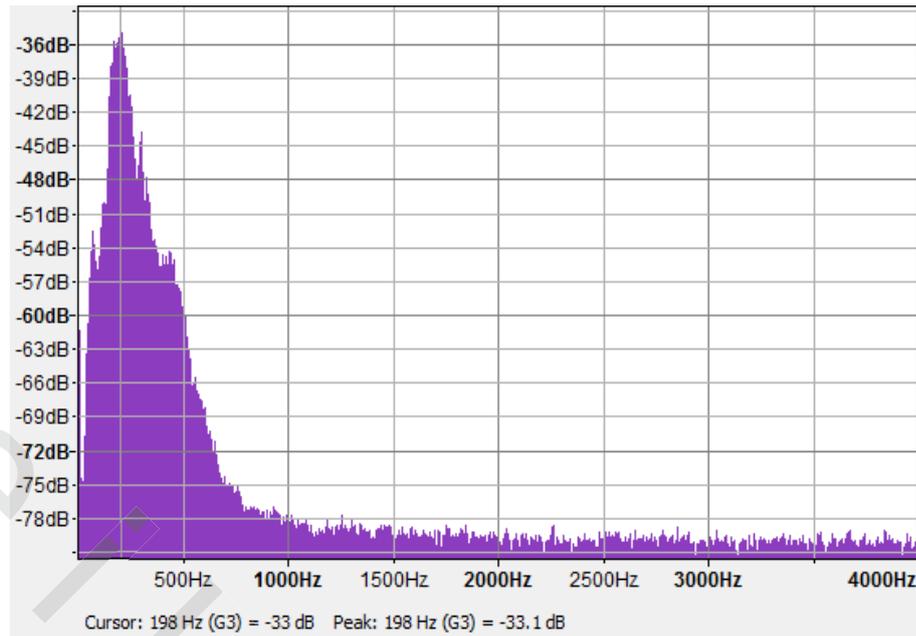
Fig. 93: The frequency domain of wheezing

Its long duration, typically more than 100 ms, allows its musical quality to be discerned by the human ear. The wheeze appears as sinusoidal oscillations with sound energy in the range of 100 to 1000 Hz.
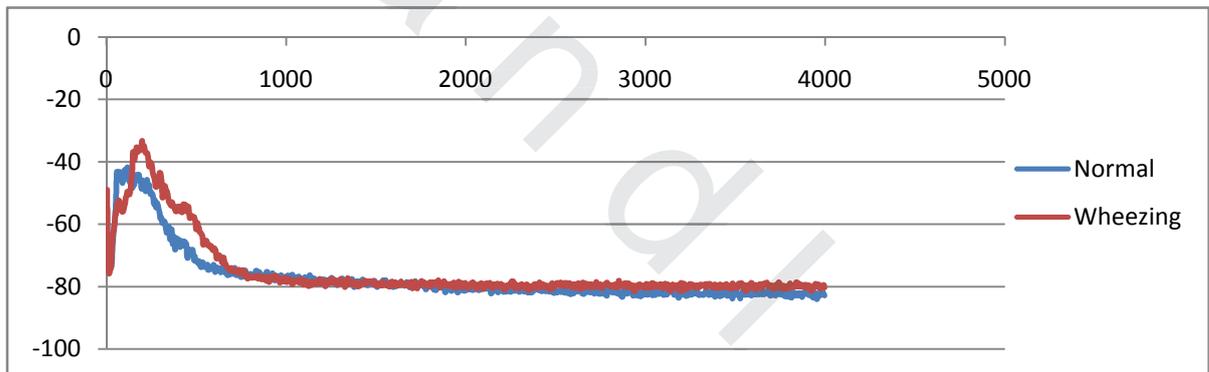
Fig. 94: Normal lung sound Vs wheezing

5.2 Applications of Active Technique for the analysis of Sound passing through balloon model (lung Phantom):

The injected fluid flowed to the bottom of the balloon due to gravity and accumulate at the microphone connected to channel I placed under the balloon. The experiment showed that as the quantity of fluid increases, the received acoustic signal amplitude increase, and the microphone connected to channel II had no response. Sound signal with a frequency of 700 Hz was injected onto the Lung model. The output signal was first monitored at a digital storage oscilloscope for displaying a numerical amplitude values for each water quantity to calculate the attenuation and the attenuation coefficient of the sound signal (figures 95, 96).
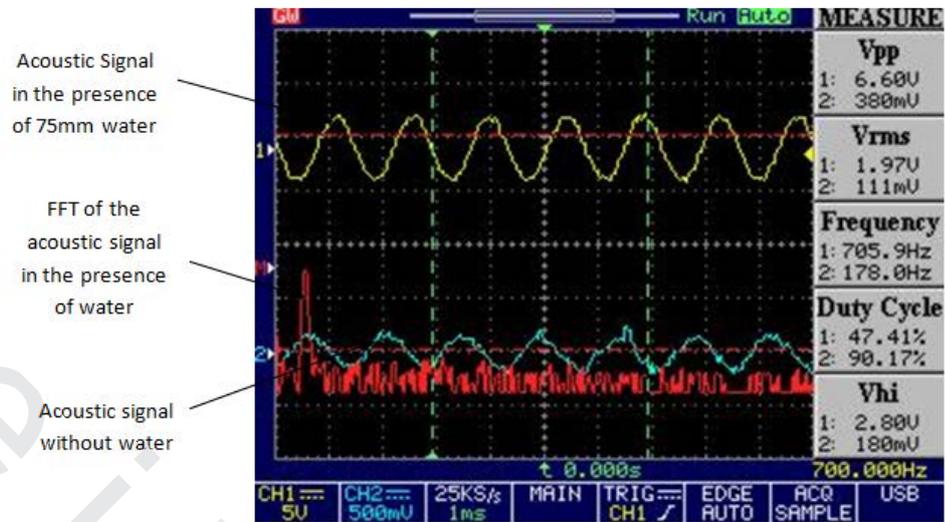
Fig. 95: The output signals of the two stethoscopes displayed from a digital oscilloscope
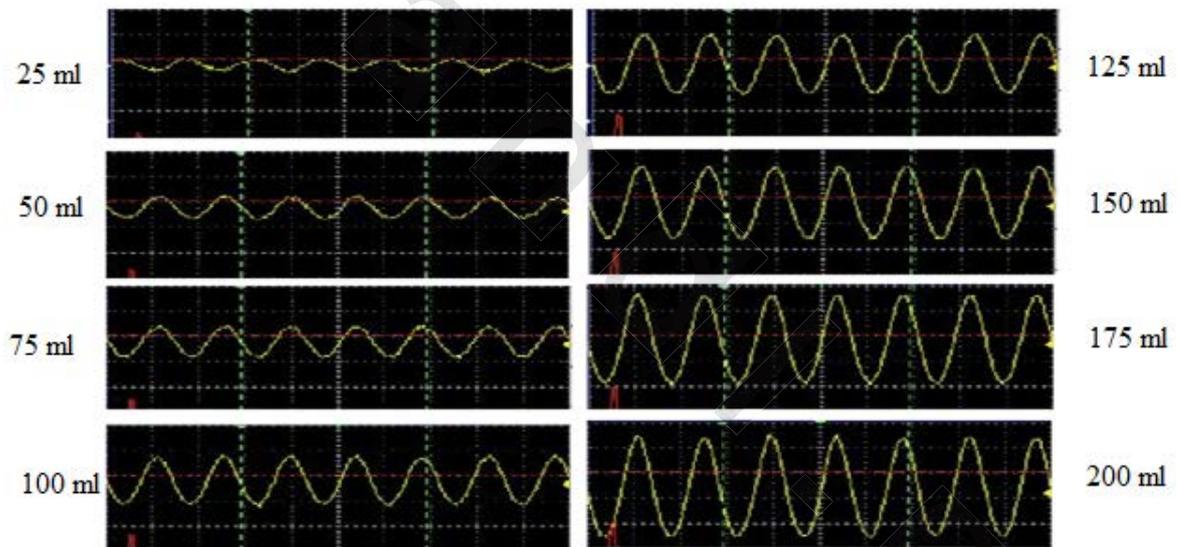
Fig. 96: The increasing of signal amplitude in time domain for each water quantity

Fig. 97 shows a linear relationship between the water volume and the signal amplitude. As the water volume increases, the signal amplitude increases too.
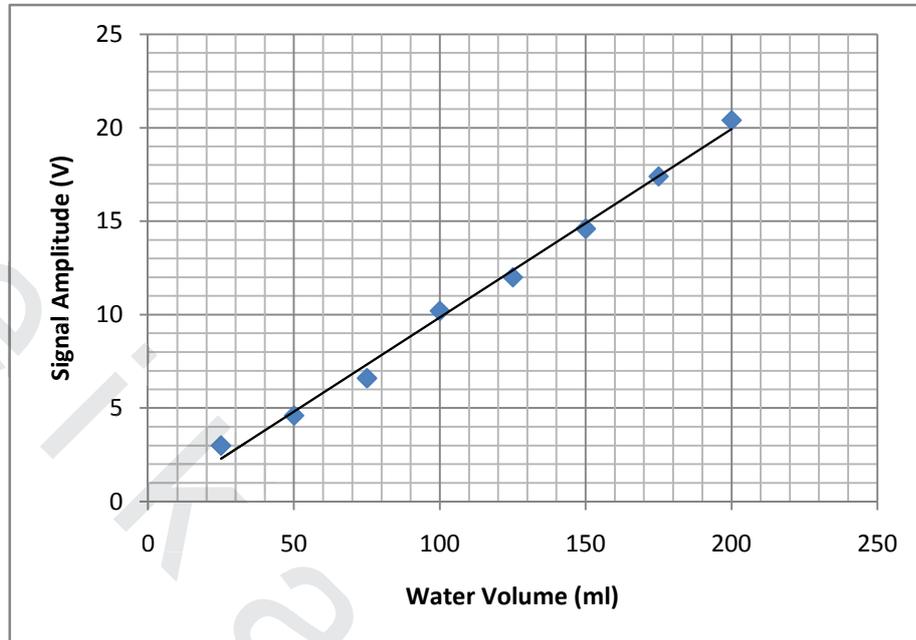
Fig. 97: Relation between water volumes and signal amplitude

Fig. 98 shows a linear relationship between the water volumes in ml and the attenuation of the sound signal in dB. As the water volume increases, the attenuation increases.
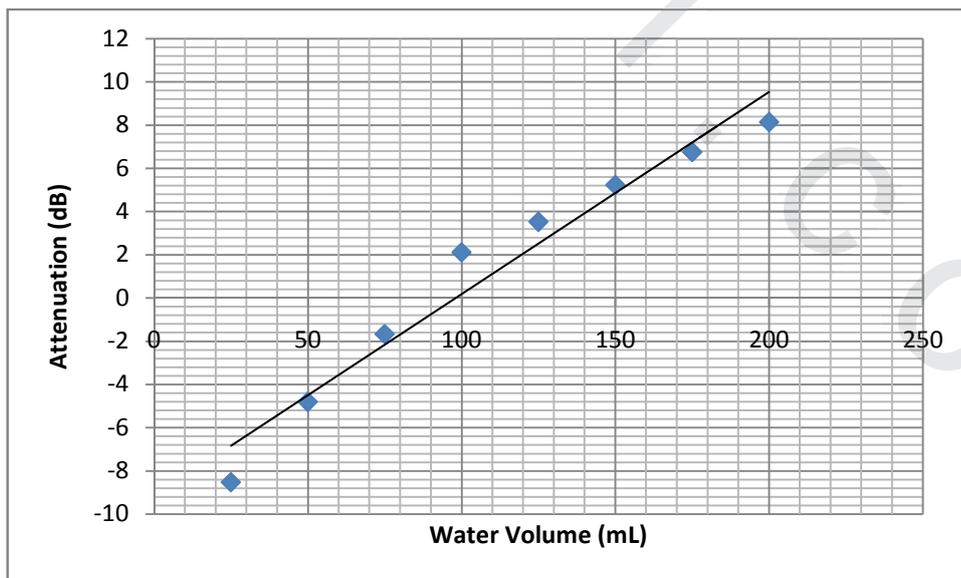
Fig. 98: Relation between water volumes and the attenuation

Fig. 99 shows a linear relationship between the water volumes in ml and the percentage of the change in attenuation coefficient. As the water volume increases, the percentage change in attenuation coefficient increases.
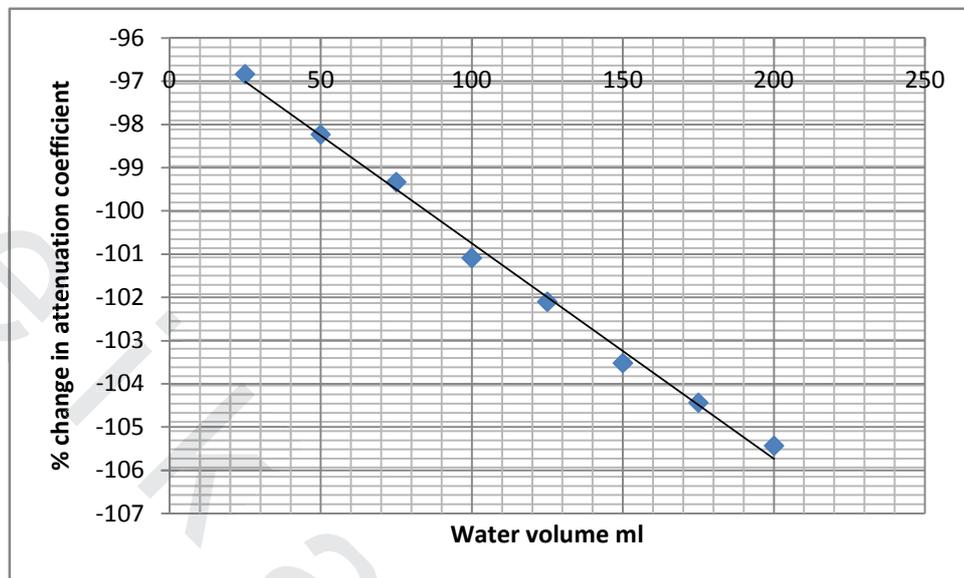
Fig. 99: Relation between water volumes and % change in attenuation coefficient

5.2.1 Software analysis:

5.2.1.1 Water quantities:

The output sound signal was interfaced to a PC by multi track audio editor (Audacity) software, which to convert the time domain of a signal to its frequency domain to compute discrete Fourier transform (DFT) by the fast Fourier transform (FFT) analysis (figures 100- 114).

Cursor: 706 Hz (F5) = -59 dB   Peak: 698 Hz (F5) = -50.6 dB
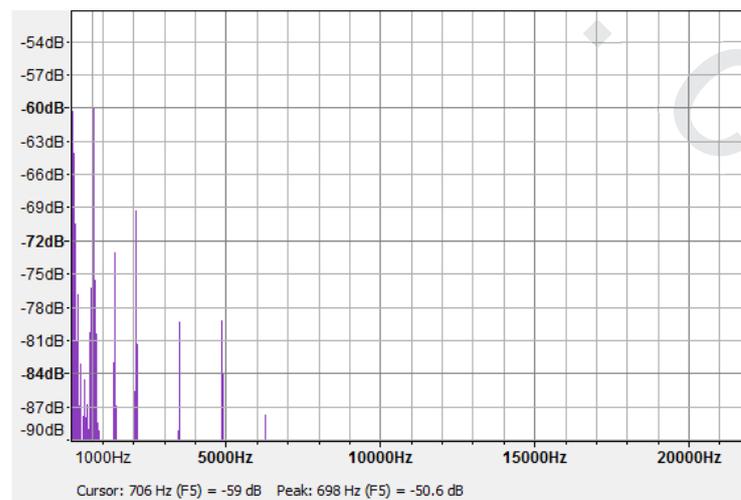
Fig. 100: The frequency domain without water
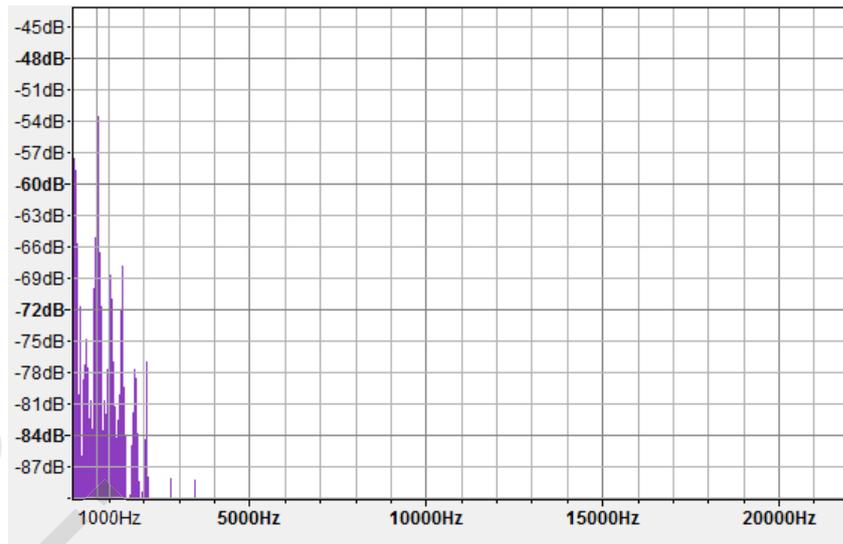
Fig. 101: The frequency domain of 15 ml water
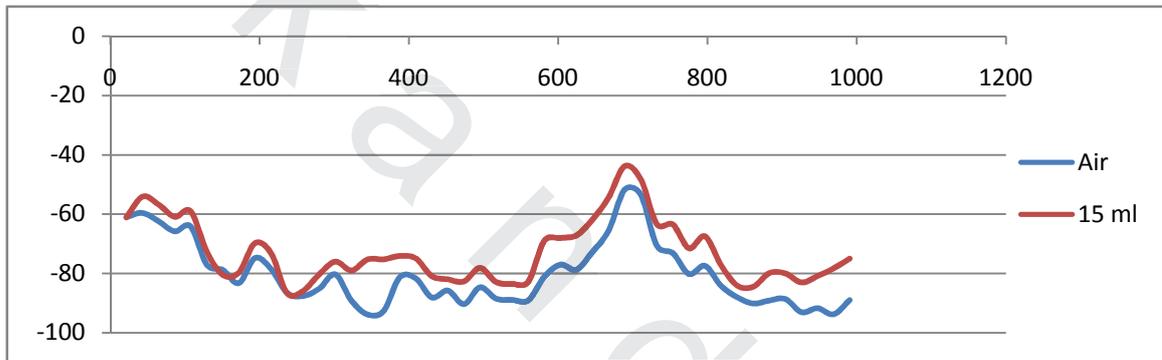
Fig. 102: Air Vs 15 ml of water

Cursor: 706 Hz (F5) = -45 dB   Peak: 691 Hz (F5) = -37.5 dB
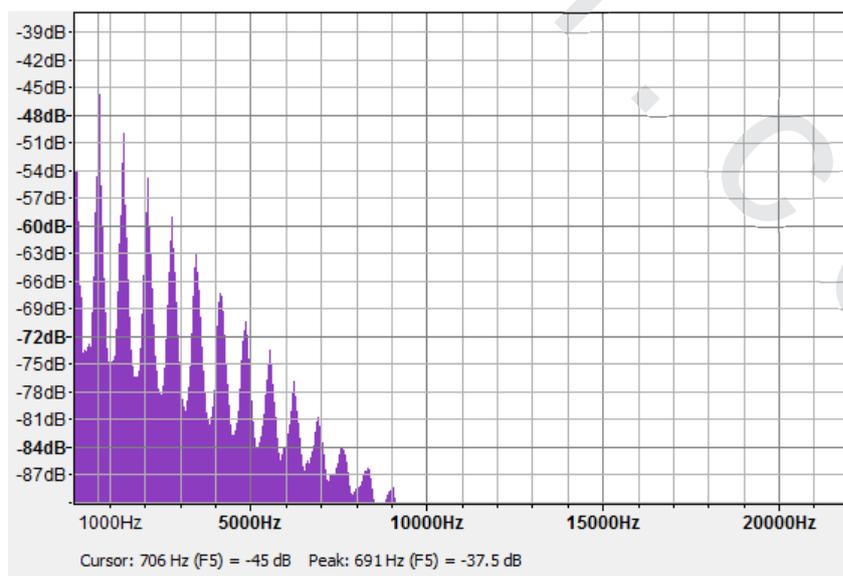
Fig. 103: The frequency domain of 25 ml of water
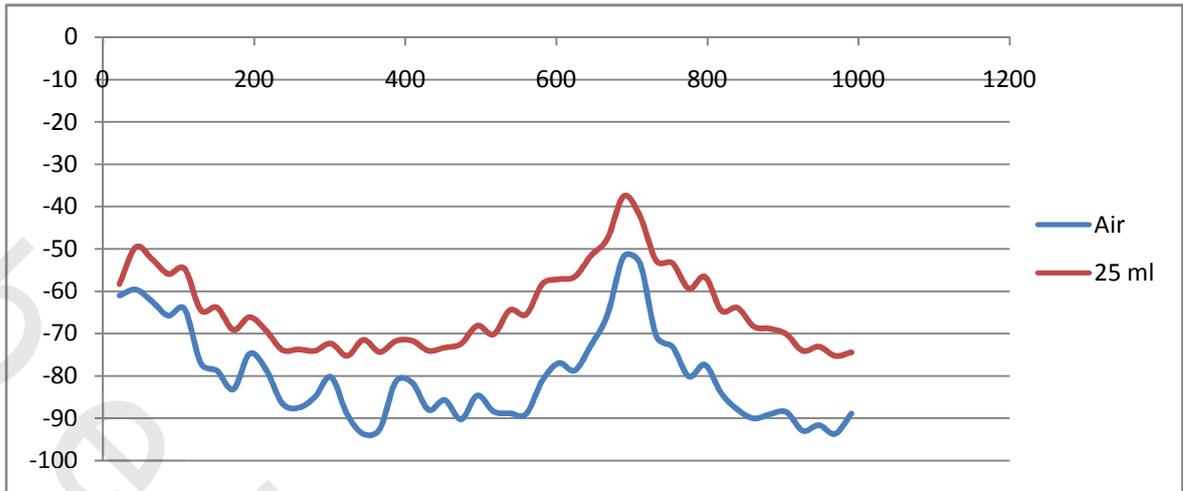
Fig. 104: Air Vs 25 ml of water

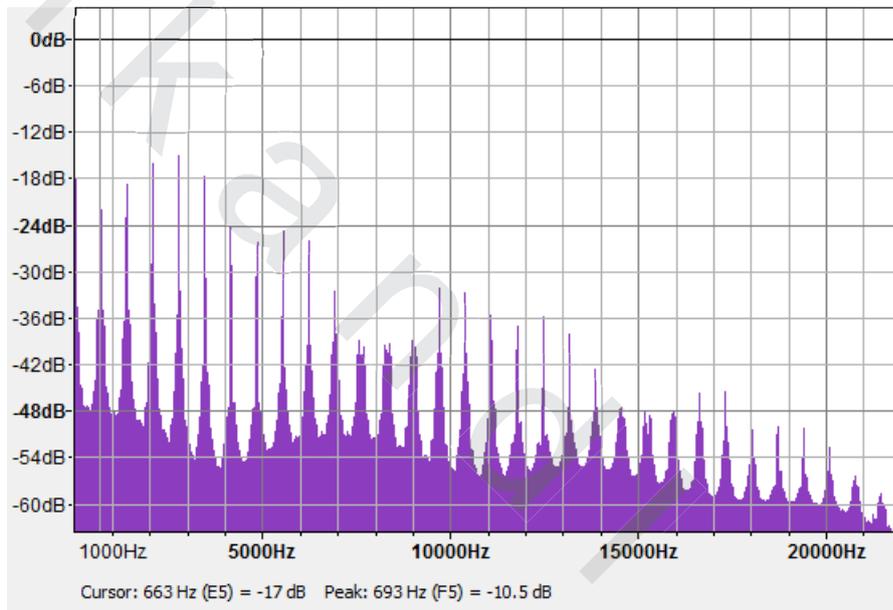Cursor: 663 Hz (E5) = -17 dB   Peak: 693 Hz (F5) = -10.5 dB

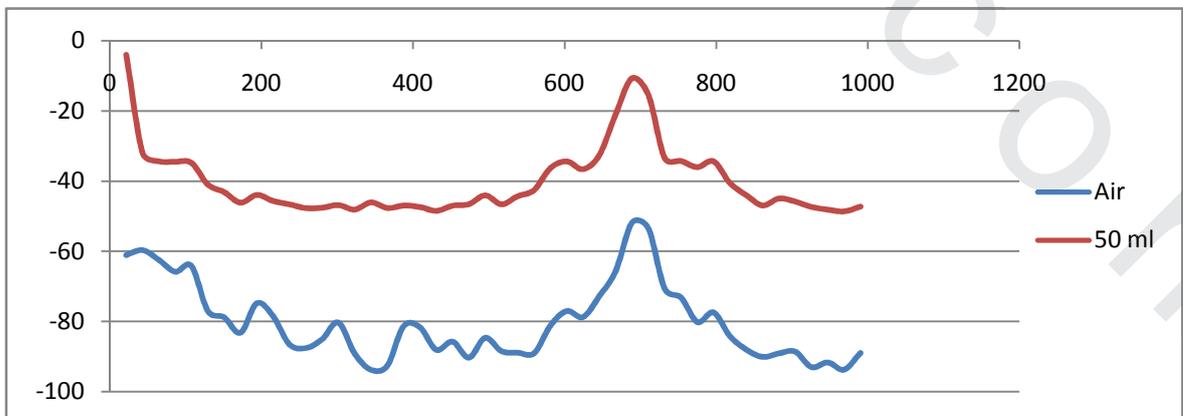**Fig. 105:** The frequency domain of 50 ml water

Fig. 106: Air Vs 50 ml of water
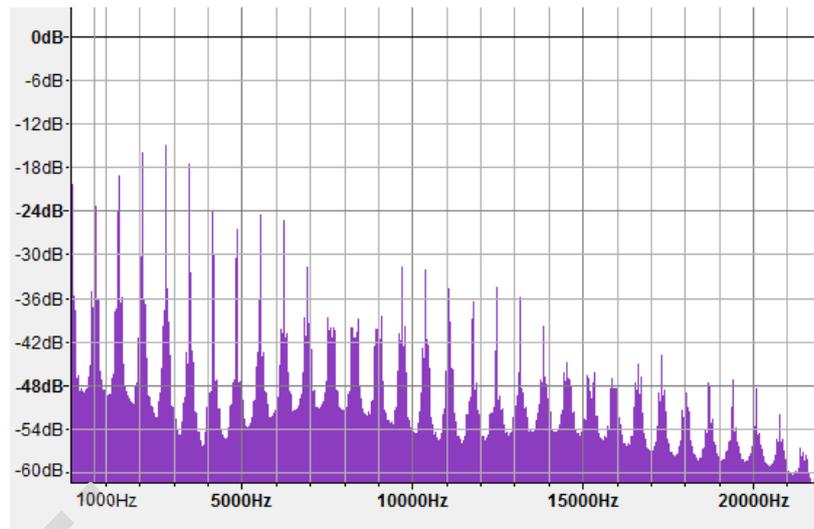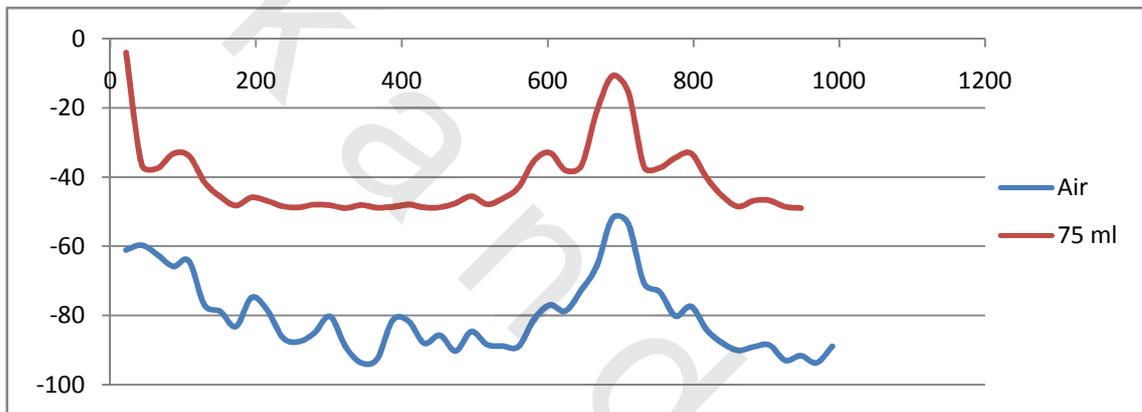
Fig. 107: The frequency spectrum of 75 ml of water

Fig. 108: Air Vs 75 ml of water

Cursor: 663 Hz (E5) = -13 dB   Peak: 695 Hz (F5) = -4.2 dB
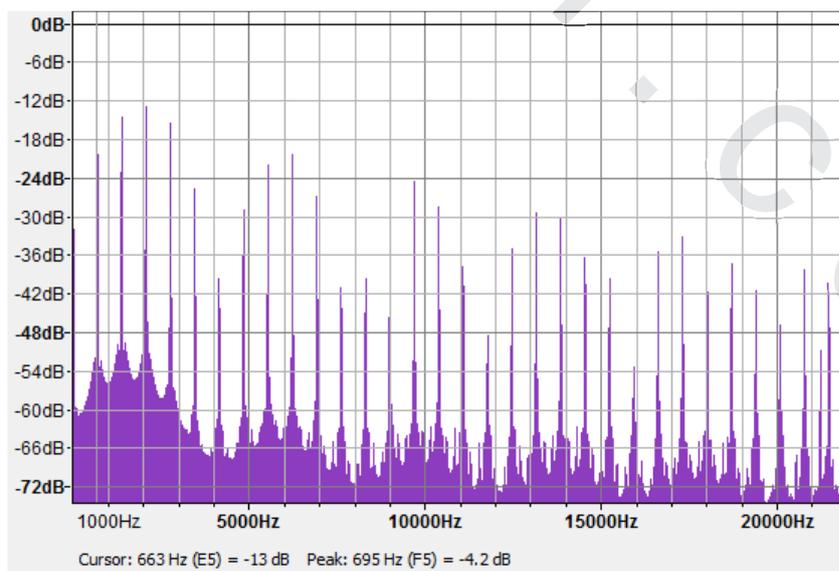
Fig. 109: The frequency domain of 110 ml of water
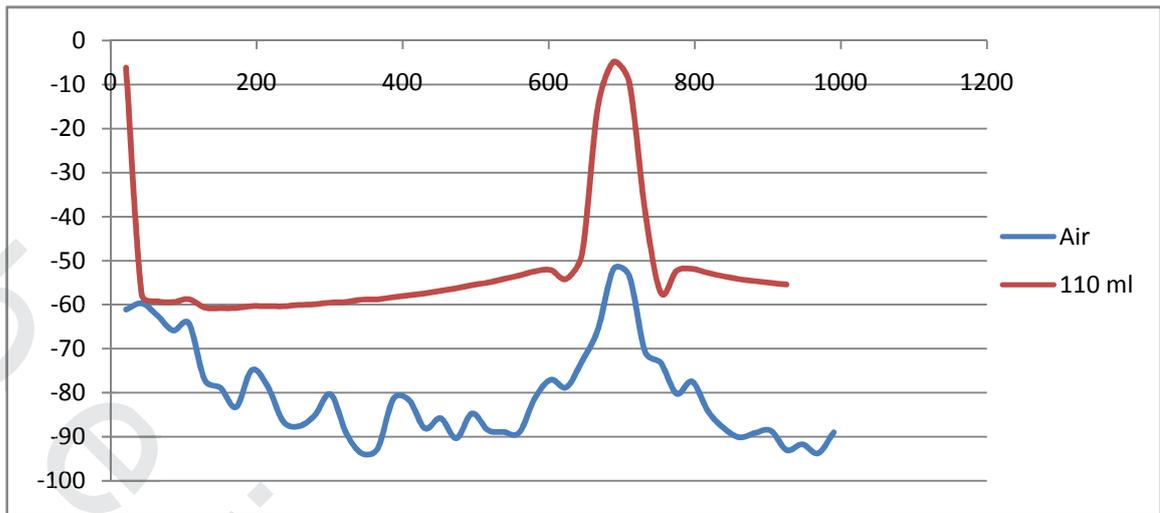
Fig. 110: Air Vs 110 ml of water

5.2.1.2 Air, liquid, and gel at the same quantity:
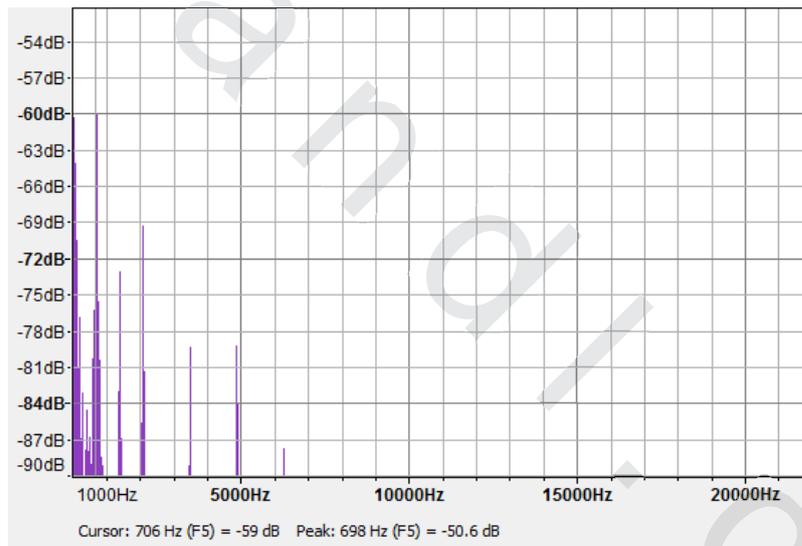

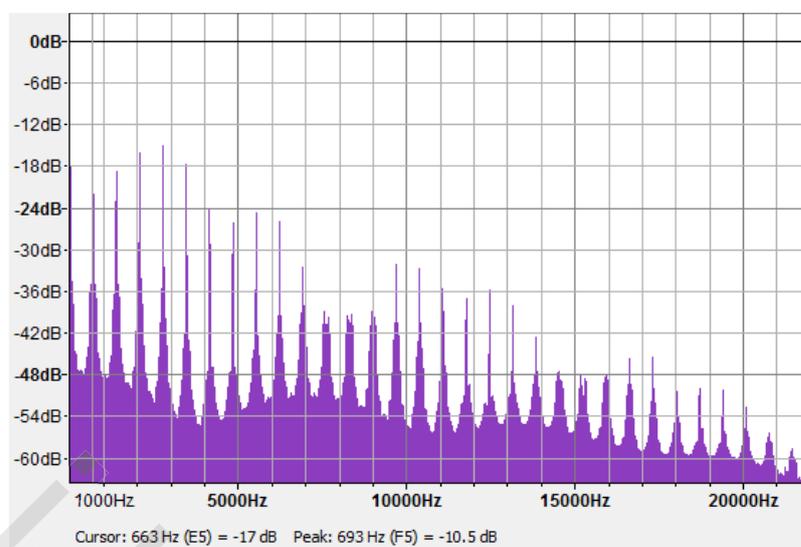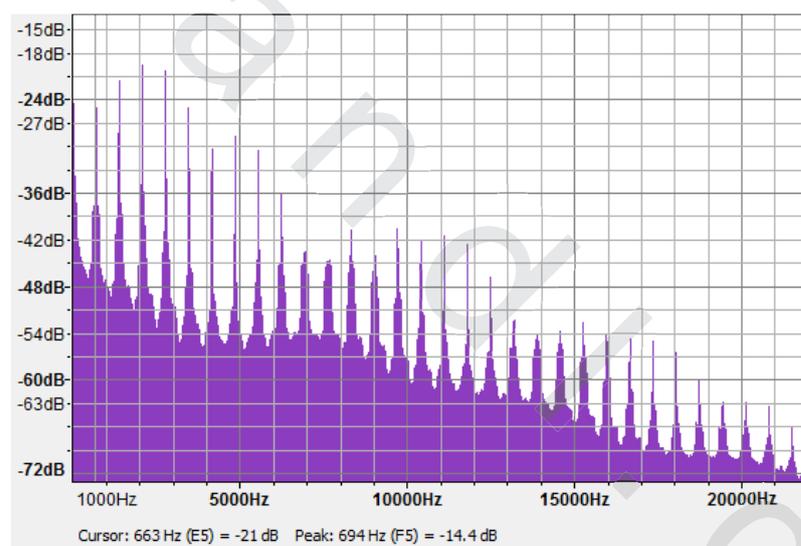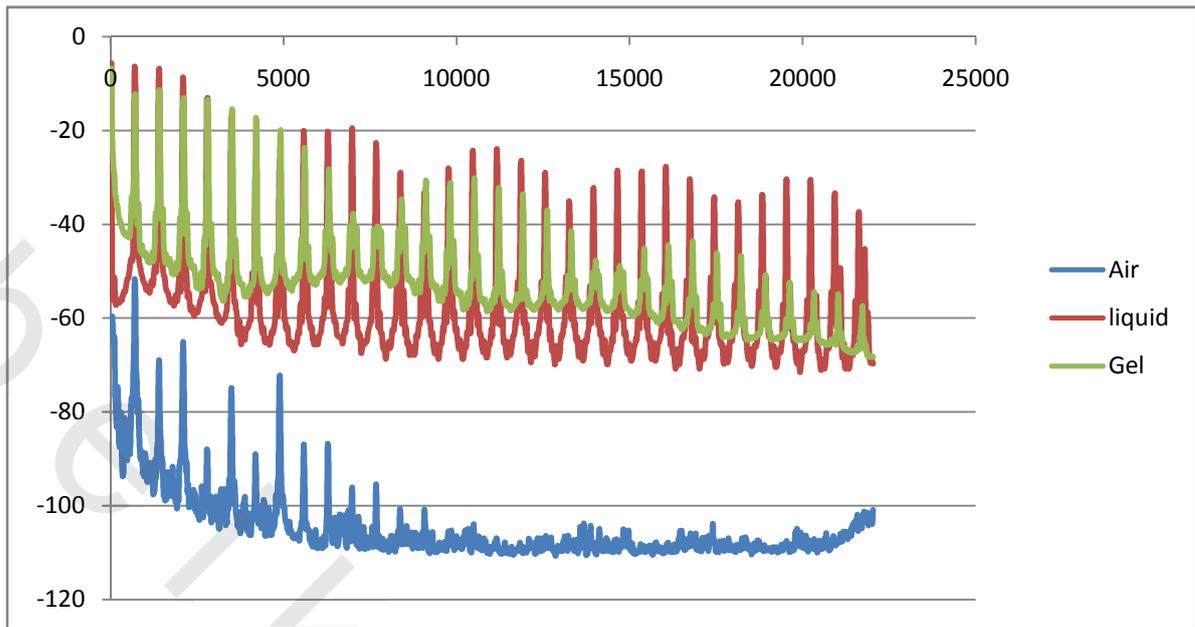Cursor: 706 Hz (F5) = -59 dB   Peak: 698 Hz (F5) = -50.6 dB

Fig. 111: The frequency domain of air

Fig. 112: The frequency domain of 50 ml of water

Fig. 113: The frequency domain of 50 ml of ultrasonic gel

Fig. 114: Air, water Vs ultrasonic gel